Journal of Materials Chemistry C

Accepted Manuscript

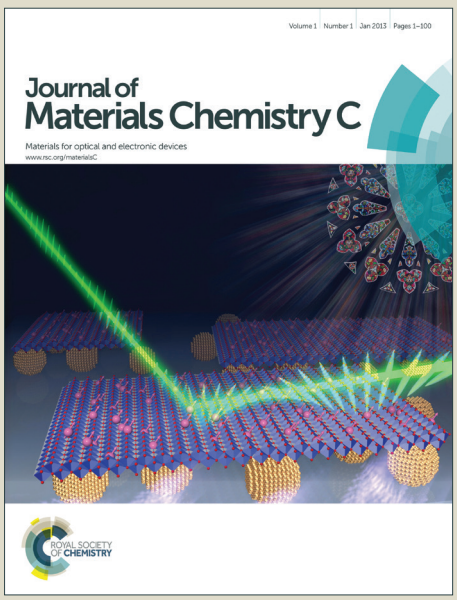

ROYAL SOCIETY OF CHEMISTRY

www.rsc.org/materialsC

Journal Name

RSCPublishing

ARTICLE

Beyond perylene diimides: synthesis, assembly and function of higher rylene chromophores

Cite this: DOI: 10.1039/x0xx00000x

Long Chen,* Chen Li, and Klaus Müllen*

Received 00th January 2012,
Accepted 00th January 2012

DOI: 10.1039/x0xx00000x

www.rsc.org/

Perylene diimides are among the most important chromophores in dyestuff chemistry. They do not only have excellent thermal, chemical and photochemical stability, high absorption coefficients and fluorescence quantum yields but they permit various chemical functionalization as well. Over the last decades, academic and industrial interest in this class of chromophores has steadily increased due to their favourable properties and potential application in various research fields like organic electronics, biochemistry, photophysics and supramolecular chemistry. Higher rylene diimides dyes (e.g. **2**-**6** in Figure 1), however, are still in their infancy and must be further explored by combining more research efforts of chemists, physicists, biologists, and material scientists since these dyes possess unique optical, electrochemical, and electronic properties. One of the main obstacles in such rylene based dyes seems to be their synthetic challenges. Thus, in this feature article, we summarize the latest advances in the field of rylene diimide dyes focusing on synthetic strategies toward their preparation. The self-assembly behaviour and applications of larger rylene chromophores are discussed as well.

1. Introduction

Rylene is a series of polycyclic hydrocarbons based on naphthalene units that are linked in the *peri*-position. Presuming such a chromophore system as an oligomer, one might also consider rylene dyes as oligo(*peri*-naphthalene)s (aromatic cores of **1**-**6**). Rylene based imides bearing one or two six-membered carboxylic imide rings, which are fused at the terminal naphthalene units, are widely used as dyes and pigments in a variety of applications owing to their outstanding chemical, thermal, and photochemical stability.[1] The most intensively investigated representatives are the naphthalene-1,8:4,5-tetracarboxylicdiimides (NDIs) and perylene-3,4,9,10-tetracarboxylic diimides (PDIs) which are applied in the fields of colorants and lacquers, particularly in the car industry,[2] and also as key chromophores for high-tech applications such as organic photovoltaics,[3] organic field-effect transistors,[4] bio-labeling,[5] sensors,[6] single molecular spectroscopy,[7] and supramolecular assemblies.[8] The synthesis, organization, and applications of various NDI and PDI derivatives were already reviewed a number of times.[3-4, 9] While PDIs have been intensive investigated, higher rylene diimides (RDIs) remained largely ignored up to now,[10] probably due to the challenging synthesis and their poor solubility originating from strong π-π stacking making the synthesis, processing, and characterization of this class of materials rather difficult. In this feature article, we focus on the synthetic strategy, self-assembly behavior at different length scales, and functionalities of rylene diimides that are larger than PDIs.

2. Synthetic Concepts

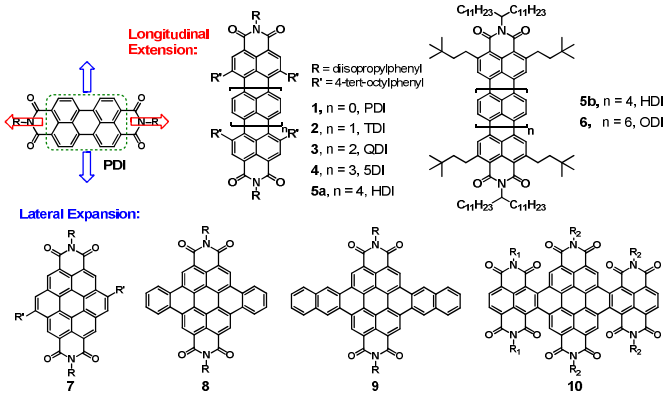

Figure 1. Representative examples for illustration of conjugation enlargement of PDI by the "longitudinal extension" and "lateral expansion" strategies.

Several concepts have been developed to explore higher rylene diimide analogues of PDI. These include: (1) extension of the π-conjugation in a longitudinal or lateral manner; (2) introduction of donor units into the perylene core to enhance the intramolecular charge transfer effect; (3) formation of stable quinoidal structures; (4) covalent linkage with multiple rylene imides to build up a multichromophore system; (5) fusion with other large π-conjugated systems (e.g. porphyrin). This new family of dyes not only exhibits light absorption in the near-infrared (NIR) range, but also features increased intermolecular π-π stacking, thus favoring charge carrier transport.[11] In contrast, when the π-system is expanded at the *bay*-positions (i.e. lateral expansion along the short axis), dyes with

hypsochromically shifted absorption are obtained.[12] In this section, we are going to discuss the basic concepts and the major progress toward the synthesis of higher RDI analogues (i.e. larger than PDI) in recent years, according to the aforementioned categories.

2.1 Conjugation Enlargement

2.1.1 Longitudinal extended perylene diimides

a) Higher rylene diimides

The astonishing properties of PDIs brought chemists to explore its higher analogues having NIR absorption such as terrylenetetracarboxylic diimides **2** (TDI),[13] quaterrylenetetracarboxylic diimides **3** (QDI),[14] pentarylene-tetracarboxylic diimides **4** (5DI),[15] and hexarylenetetracarboxylic diimides **5** (HDI).[15] For example, we reported the synthesis of QDI in 1995, of TDI in 1997 and of higher 5DI and HDI in 2006 as well. Although these syntheses have been reported for nearly twenty years, higher rylene diimides have remained to be ignored and poorly investigated. The most important building block toward higher rylene diimides is perylene-3,4-dicarboxylic acid monoimide **11** (PMI) which was obtained from the readily available perylene-3,4,9,10-tetracarboxylic acid dianhydride under harsh imidization conditions in melting quinoline at the presence of $Zn(OAc)_2$.[16] The first two higher homologues in the family of RDIs, i.e. TDI and QDI, were synthesized from naphthalene monoimides and perylene monoimides, either by cross coupling reactions and subsequent dehydrogenation[13a, 14a] or by a ''one-pot'' base-promoted cyclization process.[13b, 14c] Thus, PMI boronic ester **13** was first coupled with 4-bromonaphthalene monoimide *via* Suzuki coupling reaction providing a dyad **14**, which was then cyclodehydrogenated in molten KOH to give

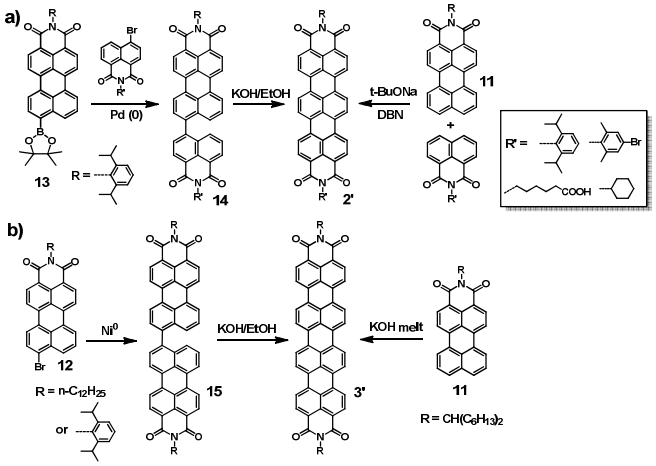

Scheme 1. Two typical synthetic routes toward TDI and QDI.

TDI **2'** (Scheme 1a). Alternatively, **2'** was obtained by direct coupling and fusion of PMI **11** with naphthalene monoimide (NMI) in a "one-pot" reaction at the presence of 1,5-diazabicyclo[4.3.0]non-5-ene (DBN) and *t*-BuONa. The use of an excessive amount of NMI avoided direct fusion of PMI which could have led to unwanted formation of QDI; resulted TDI was easily separated from the side product PDI (fusion of NMI) by rinsing with ethanol exploiting their different solubility. The advantages of this specific route are both the ease of TDI upscaling and avoidance of tedious column chromatography purification. Similarly, QDI **3'** was prepared either by a two-step process *via* homo-coupling of PMI-bromide **12** to bis-PMI **15** followed by cyclodehydrogenation under basic conditions, or by a "one-pot" direct fusion of two PMI **11** using molten KOH (Scheme 1b).[14c]

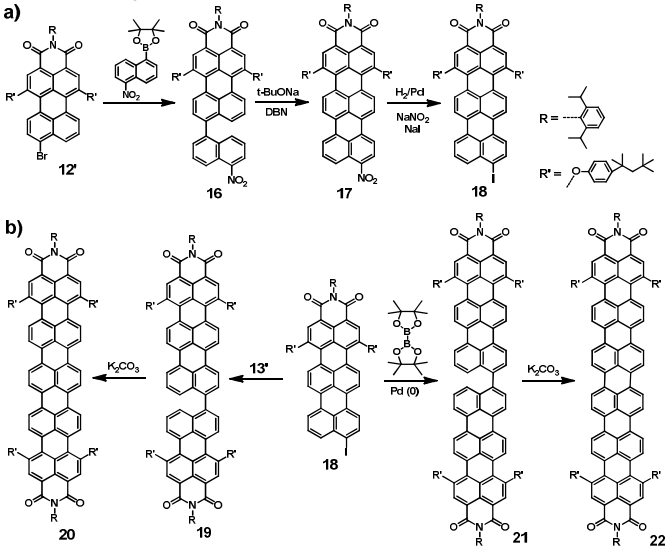

Scheme 2. The "nitronaphthalene method" synthetic route for 5DI (**20**) and HDI (**22**).

Two different concepts were developed for the synthesis of the next two members of the RDIs family: penta- and hexarylene diimides (5DI **20** and HDI **22**).[15] The first concept uses the so called "nitronaphthalene method", starting from the coupling product of 5-nitronaphthalene pinacol boronic ester and *bay*-substituted PMI-bromide **12'** (Scheme 2a). The bisaryl compound **16** was then cyclized to **17** under drastic basic conditions, reduced to its amine analogue and finally transformed into the iodo terrylene monoimide (TMI) **18** by Sandmeyer reaction. HDI **22** was obtained by homo-coupling of **18** followed by subsequent cyclodehydrogenation. Similarly, the coupling of **18** with *bay*-substituted PMI-boronic ester **13'** and subsequent planarization afforded the pentarylene diimide (5DI) **20** (Scheme 2b). This "nitronaphthalene" method, however, usually suffers from the overall low yield, especially in the Sandmeyer reaction. Thus, an alternative method toward the synthesis of 5DI and HDI was developed: the "bisbromorylene method". It involves the generation of triaryl precursor molecules, which was then under subsequent cyclodehydrogenation to afford the 5DI and HDI, respectively.[15] Further explanation of the "bisbromorylene method" will be given in more detail in the following two examples of planar HDI' (**5a**) and ODI (**6**) (Scheme 3).

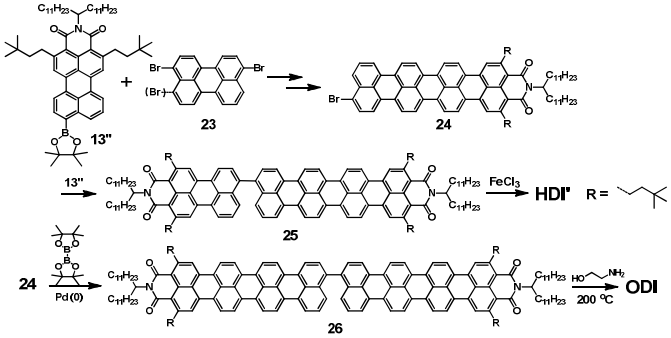

Scheme 3. The "dibromorylene method" synthetic route toward planar HDI' and ODI.

Most recently, we extended the core of rylene diimides longitudinally to octarylene diimide (ODI) with a length of approximately 4 nm.[17] Conventional strategies of making these higher RDIs soluble comprise the introduction of four *tert*-octyl phenyl groups to the *bay*-positions and two diisopropylphenyl groups at the two imides termini. Apart from that, we used an *ortho*-functionalization strategy to keep the four alkyl substituents "far" away from the central core. This method not only results in HDI' and ODI having high solubilities, but also maintains planarity of the aromatic core. The synthetic routes toward HDI' and ODI are shown in Scheme 3. Selective Suzuki coupling of the inseparable 3,9(10)-dibromo perylenes **23** with the PMI-boronic ester **13''**, bearing a long swallow-shaped alkyl chain ($C_{23}H_{47}$) and two 3,3-dimethyl-1-butyl chains at the *ortho*-positions, generated the key building block bromo quaterrylene monoimide **24** after cyclization. Suzuki coupling of **24** and **13''** led to the biaryl **25** which could be facile cyclodehydrogenated by ethanolamine to form planar HDI'. The dimerization of **24** in the presence of bis(pinacolato)diboron and Pd(0) catalyst afforded the bis-QMI **26** which, however, could not be dehydrogenated by the aforementioned conditions (K_2CO_3, $FeCl_3$ or DBN/*t*-BuONa). In the presence of $Sc(OTf)_3$ and DDQ, the dehydrogenation of **26** was smoothly accomplished in toluene.

To achieve sufficient solubility of these large rigid rylene diimide dyes, phenoxylation of 4-isooctylphenol with a dye possessing halogens at the bay positions is most common performed. It is noteworthy to mention that phenoxylation not only increases the solubility of RDIs but also induces a fine tuning of their molecular orbital energy levels due to electron donating effects of phenoxy groups. This is accompanied by an additional bathochromic shift of the absorption maximum. On the other hand, bathochromic shifts of the absorption maxima by approximately 100 nm per naphthalene unit are usually obtained by conjugation extension from PDI to HDI. For example, PDI **1**, TDI **2**, QDI **3**, 5DI **4** and HDI **5** (Figure 2a) exhibit absorption maxima at 580, 677, 762, 877 and 953 nm, respectively, and therefore appear bright orange, blue, green, light green and light yellow in solution. Also, almost linear increase of the extinction coefficient for rylene homologues (from PDI to HDI, Figure 2b) was observed. In contrast, the observed absorption maximum of ODI is 1007 nm which is roughly 100 nm lower than expected, most probably due to the H-aggregation of ODI even in extremely diluted concentration (e.g. 10^{-7} mol/L). Strong aggregation in such diluted concentrations was corroborated by STM measurement, which will be discussed later on.

b) Aminoanthraquinone-rylene dyes

An aminoanthraquinone-rylene conjugated system **28** that includes heteroatoms was synthesized starting from monoimides and 1,5-diamoninoanthraquinone.[18] Like RDI, **28** contains two dicarboxyl imides in the two terminal positions of the conjugated backbone as well, however, bears an anthraquinone core in the middle which enables intramolecular hydrogen bonding of two ketone groups of the anthraquinone with the adjacent secondary amine protons. The intramolecular H-bonding also largely contributes to the bathochromic shift in absorption toward the NIR region. Two equivalents of the rylene monoimides (NMI or PMI) **12a–b** (bromo-substituted in the *peri*-position) were each coupled with 1,5-diaminoanthraquinone

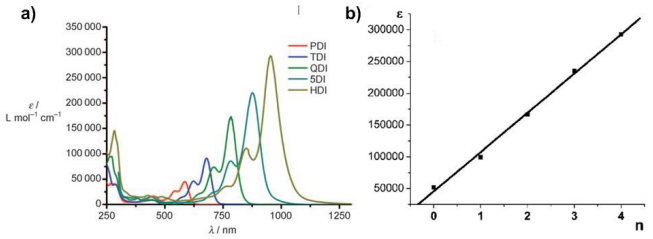

Figure 2. a) Comparison of absorption spectra of rylene diimides. b) Correlation between the number of naphthalene units and the extinction coefficient. Adapted with permission from Ref. [15], Copyright 2006, Wiley-VCH.

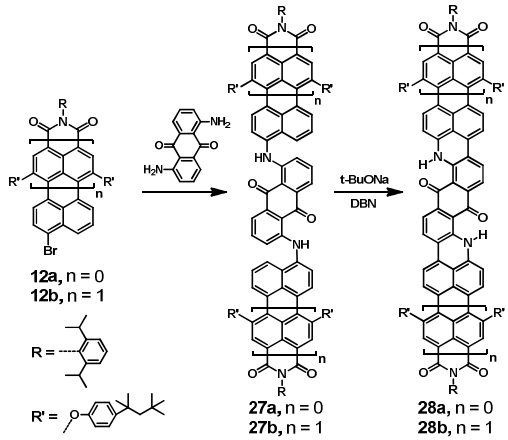

Scheme 4. Synthesis of aminoanthraquinone based rylene diimides **28**.

under $Pd(PPh_3)_4$ catalyzed amination (Scheme 4). The intermediates **27a–b** obtained by amination, were further planarized by mild base-promoted cyclization and provided the NIR absorbers **28a–b** in high yields. The absorption spectrum of the deep green dye **28a** exhibits two absorption bands (λ_{max} = 440 nm and 778 nm). In the case of the higher analogue **28b**, a similar absorption profile was detected (λ_{max} = 618 nm and 1106 nm) resulting in a blue color due to the sharp absorption band at 618 nm.

2.1.2 Lateral expanded perylene diimides

Core-expansion of PDIs includes annulation of benzene rings and heterocycles in the *bay*-region of the perylene core.[19] The key building block for core expansion of PDI is 1,7-dibromo-PDI **29** (Schme 5a), which can be obtained by bromination of perylenedianhydride in concentrated sulphuric acid with bromine[19a] followed by imidation reaction with alkyl- or aryl-amines. These compounds allow easy access to a different class of chromophores, including the coronene diimides (CDI) **7**,[12a, 19b] dibenzocoronene diimides **8**,[20] dinaphthocoronene diimides **9**[19c] (Figure 1). For the synthesis of CDI **7,** 1,7-dibromo-PDI **29** was coupled with various 1-alkynes by Sonogashira reaction to afford the bis(alkynyl)-substituted perylene-3,4:9,10-bis(dicarboximide)s **30**, which was subsequently treated with 1,8-diazabicyclo[5.4.0]undec-7-ene (DBU) through a base promoted cyclization reaction to yield CDI **7** as yellow compound in almost quantitative yield (Scheme 5a). With appropriate alkyl substitution, the CDI **7** formed discotic mesophases. CDI **7** fluoresces with an intense green-yellow color at a maximum of 517 nm. The absorption bands of **7** displayed a blue-shift (ca. 35 nm) with respect to of its precursor **30** and a red-shift (ca. 89 nm) when compared to the parent coronene (428 nm).[21]

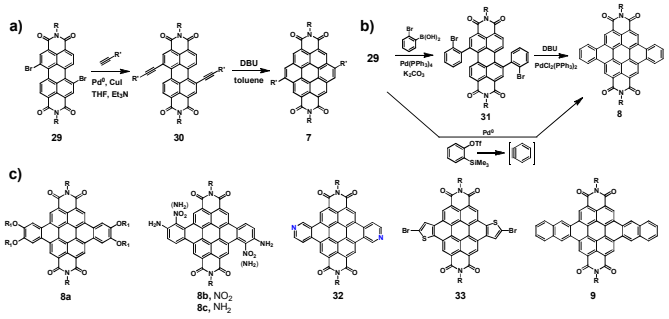

Scheme 5. a) Synthesis of coronene diimides **7**; b) Synthesis of dibenzocoronene diimides **8**; c) The latest examples of extended coronene diimides **8**, **9, 32**-**33**.

Further expansion of a perylene core from coronene to dibenzocoronene dyes was achieved by an alternative route involving Suzuki coupling and subsequent palladium-catalyzed dehydrohalogenation reactions. As illustrated in Scheme 5b, Suzuki coupling of **29** with 2-bromophenylboronic acid afforded **31**, which was further converted to a light brown solid dibenzocoronene diimide **8** in 46% yield by a palladium-catalyzed cyclodehydrohalogenation[22] with DBU as base in dimethyl acetamide.[20] To optimize this synthetic route regarding large-scale productions, the procedure was simplified by core-extension of the *bay*-region of PDI via a one-step Diels–Alder cycloaddition.[20] The reaction of the commercially available 2-(trimethylsilyl)phenyl trifluoromethanesulfonate and *N,N'*-dioctyl-1,7-dibromoperylene diimide **29** under the conditions described above afforded dibenzocoronene diimide **8** in high yield (80%). Recently, Yang et al. reported a tetraalkoxylated dibenzocoronenediimide **8a** which was synthesized via a two-step route, and exhibited thermotropic liquid crystalline behavior (Scheme 5c).[23] Most recently, Xiao and coworkers used the 3-nitro-4-aminophenyl boronic acid in the Suzuki coupling with **29** followed by a light-promoted dehydrogenation to afford the dinitro-diamino-substituted dibenzocoronene diimide **8b**.[24] Subsequent reduction of **8b** afforded the versatile building block tetramino-dibenzocoronene diimide **8c** which could be condensed with various aromatic diketones or tetraketones in order to generate much larger chromophores and organic semiconductors.[24] Wang et al. reported a nitrogen annulated CDI analogue **32**, where a 4-pyridine boronic acid was chosen as precursor due to its better stability than 2-pyridine boronic acid.[19d] The fused target **32** was obtained by *in-situ* cyclodehydrogenation of the Suzuki coupling intermediate *via* exposure to ambient light. In addition to the pyridine annulation of CDI, Facchetti and coworkers reported a thiophene-fused CDI **33**, where the two α-protons of thiophene are substituted with bromo groups.[19e] This enabled the synthesis of a series of low band gap donor-acceptor π-conjugated polymers by Suzuki,[19e] Sonogashira,[19f] and Stile[19g] polycondensation of CDI **33** with various donor molecules. Our group further extended the higher analogue of CDI using the one pot Diels-Alder cycloaddition reaction by refluxing **29** with 3-(trimethylsilyl)naphthyl-trifluormethane-sulfonate in a mixture of toluene and acetonitrile. The desired product dinaphthocoronene diimide **9** was obtained in 46% yield. **9** exhibits a broad absorption from 450 to 600 nm, leading to a bright purple-red appearance.[19c]

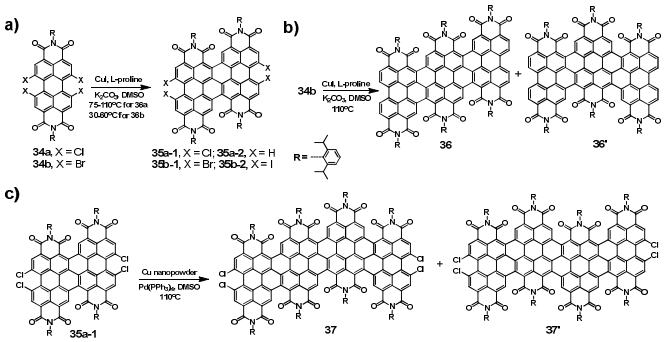

Scheme 6. Synthesis of ladder-type (ribbon like) PDI dimer **35**, trimer **36**, **36'** and tetramer **37**, **37'**.

Besides the aforementioned annulation of ethylene, benzene, pyridine, and thiophene units to the *bay*-positions of PDI, recently, a more complex core-expanded hybrid system was introduced. A series of nanoribbon-like PDI oligomers fused in the *bay*-positions were reported by Wang and coworkers.[25] In 2007, they for the first time introduced one-pot synthesis of diperylene diimide (diPDI **35a-2**) and tetrachlorinated diperylene diimide (4CldiPDI **35a-1**) from readily available 1,6,7,12-tetracholro-PDI **34a** via a domino process involving L-proline and CuI promoted Ullmann coupling and C-H transformation (Scheme 6a). The formation of **35a-1** and **35a-2** can be controlled by the reaction temperature, at lower reaction temperature (e.g. 75 °C) the 4CldiPDI (**35a-1**) was obtained, while at elevated temperature (e.g. 110 °C), dechlorination occured and afforded the diPDI (**35a-2**).[25a] By the use of the more reactive 1,6,7,12-tetrabromo-PDI (**34b**) instead of the chlorides as the precursor, the lateral fusion proceeded at a lower temperature (30 °C) and afforded tetrabromo-diPDI (**35b-1**). Slight increase of the reaction temperature to 60 °C led to a halogen-exchanged product tetraiodo-diPDI (**35b-2**).[25b] Even further increase of the reaction temperature to 110 °C and addition of cocatalyst CuI/L-proline and K_2CO_3 led to cleavage of the bromine atoms at the edge and resulted in fully conjugated tri(perylene diimides) (triPDIs) (Scheme 6b). Two structural isomers of triPDIs **36** and **36'**, which were readily separated by HPLC, were formed due to two accessible coupling positions.[25c]

Moreover, by the use of the tetrachlorinated-diPDI **35a-1** as starting material and $Pd(PPh_3)_4$ as well as nano-sized copper powder as co-catalysts at 110 °C, fully conjugated tetrachloro-tetra-PDIs were successfully obtained in 8% yield (Scheme 6c).[25d], The two isomers were separated by cyclic HPLC separation and unambiguously characterized: **37** (2%) and **37'** (6.3%). Interestingly, the electrochemistry of **37** and **37'** exhibited one two-electron and six one-electron reduction waves, which is of great interest for application in n-type semiconductors owing to an extremely low LUMO energy level of -4.65 eV for **37** and -4.68 eV for **37'**.[25d]

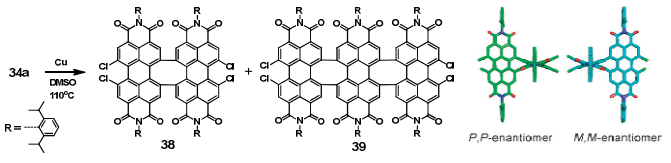

Scheme 7. Synthesis of chiral ribbon like doubly-linked oligo-perylene diimides **38**-**39**. Adapted with permission from Ref. [26], Copyright 2010, Royal Society of Chemistry.

Different from triply-linked PDI ladder type oligomers **36**-**37** which were laterally fused at the two *bay*-positions and one

ortho-position, a novel system of **38**-**39** was introduced by Wang et al. These two chiral ladder-type PDI oligomers were doubly coupled at the *bay*-positions only and were obtained via the copper mediated Ullmann coupling reactions (Scheme 7).[26] Due to the eight-membered ring formation between each PDI molecules, the molecules are highly twisted and resulting in two conformations for the dimer **38** and three conformations for the trimer **39** could be distinguished by both circular dichroism measurements and chiral HPLC.

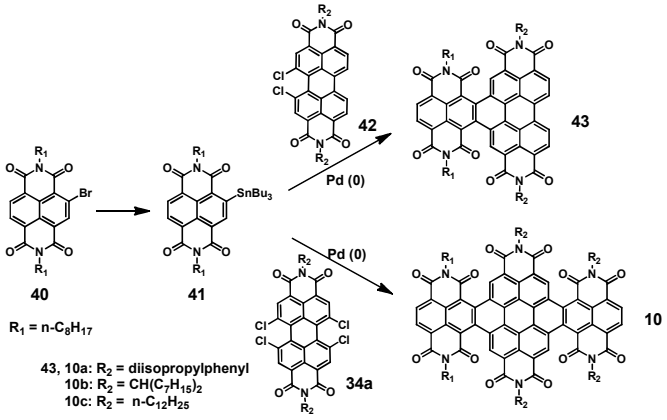

Scheme 8. Synthesis of hybrid rylene arrays (NDI+PDI) **43** and **10**.

Besides homocoupling of PDI, heterocoupling of PDI and other RDI (e.g. NDI) along the equatorial axis via Stille coupling and C-H transformation was recently reported as well.[27] The mono-stannyl NDI **41** was obtained by Stille coupling of the monobromo NDI **40** with Bu_3Sn-$SnBu_3$ in the presence of $Pd_2(dba)_3$ and P(*o*-tol)$_3$ in toluene (Scheme 8).[28] For a model reaction, 1,12-dichlorinated-PDI **42** was firstly chosen as substrate for the cross-coupling with **41** affording the NDI-PDI array **43** in 33% yield. Furthermore, reaction of readily available tetrachlorinated-PDI **34a** with **41** generated the NDI-PDI-NDI array **10** in 35-46% yield. The lateral extension of the π-system using additional NDI not only extended the absorption region toward near infrared (NIR) but also increased the electron affinity, which facilitates electron injection and transport with ambient stability. Another example of core-expanded PDI is the bisanthracene bis(dicarboxylic imide)s, as shown in Scheme 9.[29]

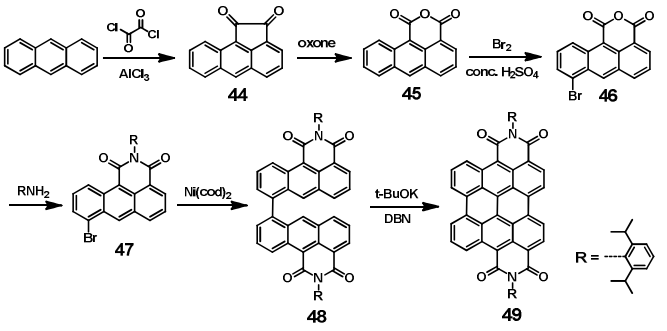

Scheme 9. Synthesis of bisanthracene bis(dicarboxylic imide)s **49**.

The bisanthracene diimide **49** can't be directly synthesized from PDI but is accessible by a multiple-step synthesis starting from anthracene. Contrary to aforementioned CDI, the bisanthracene diimide **49** exhibits an intense absorption in the NIR regions with an absorption maximum at 830 nm indicating a significant bathochromic shift of about 300 nm, compared to its PDI analogues.

2.1.3 Rylene diimides with combined longitudinal and lateral extensions

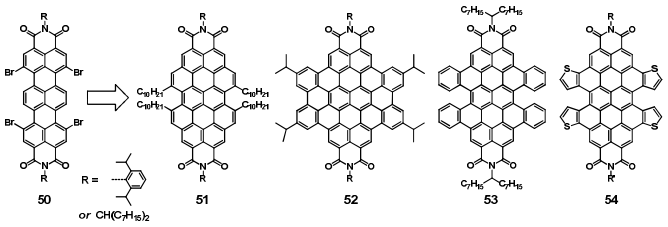

Scheme 10. Representatives of core-expanded TDIs synthesized from tetrabromo-TDI **50**.

We and other research groups further extended the core annulation of higher rylene dyes (e.g. TDI, QDI and 5DI) resulting in an enlargement of π-conjugation in both molecular axes. Several examples based on highly photostable blue TDI dyes were recently reported. The key intermediate tetrabromo-TDI **50** was prepared by bromination of TDI in boiling $CHCl_3$ in good yield (75%).[13b] Various metal-catalyzed coupling reactions such as Sonogarshira, Suzuki, and Stille coupling could be performed with this versatile building block **50** (Scheme 10). For instance, Sonogarshira coupling of **50** with 1-dodecyne yielded the tetra-ethylene substituted TDI which was directly converted to the core expanded TDI **51** by addition of DBU.[30] Similarly, Suzuki coupling of **50** with 3-isopropylphenylboronic acid produced the tetra-phenylated TDI in 63% yield, which was subsequently transformed to the large disc-shaped diimide **52** by intramolecular oxidative cyclodehydrogenation using $FeCl_3$ as oxidant.[30] Futhermore, Wang and coworkers introduced a tetrathiophene annulated TDI **54**, where a fourfold Stille coupling of **50** with 2-(trisbutylstannyl)-thiophene were performed. Subsequent cyclodehydrogenation under typical Scholl conditions using $FeCl_3$ as oxidant afforded thiophene annulated TDI **54**.[31] Our group applied the facile one-pot Diels–Alder cycloaddition, as applied for **29**, to synthesize the four benzene rings annulated TDI **53**. The four-fold palladium(0) catalyzed annulation of the tetrabromo-TDI **50** with *o*-trimethylsilyl-phenyltriflate afforded the benzannulated TDI **53**.[32] The large steric encumbrance effect between the four neighboring benzene rings at the *bay*-positions twists the molecules with torsion angles of ca. 45° or 50° resulting in two diastereomers (with up-down or butterfly conformations) which could be separated *via* standard silica chromatography. Two atropo-enantiomers of the isomer with "up-down" conformation could further be isolated by chiral HPLC. The optical and chiral properties of these three isomers were fully characterized and well-assigned. The high racemization barrier endows the two atropo-enantiomers of **53** with high thermodynamic stabilities, which is of high interest in chiral molecular switches.[33]

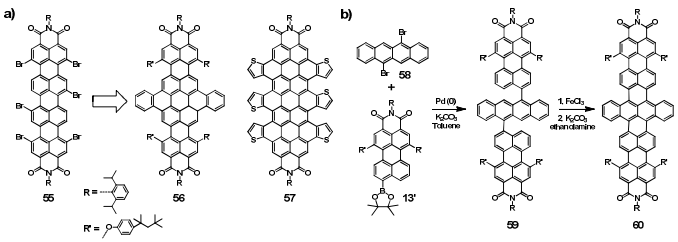

Scheme 11. a) Reported core-expanded QDIs synthesized from hexabromo-QDI **55**; b) Synthesis of core-expanded 5DI **60**.

Bromination of QDI **3** with an excess of Br_2 in chloroform at 55 °C afforded the six-fold brominated product **55**.[20]

Hexabromide **55** is more soluble than QDI due to twisting of the quaterrylene core. We observed that phenoxylation only occurred at the four bromides closest to the imide positions. The two ''inner'' bromides did not react even after longer reaction times and more drastic conditions. However, the remained two "inner" bromides were suitable for the palladium promoted benzannulation. The core expansion of QDI **55** under the same conditions as those of **29** afforded the core-expanded QDI **56** in 46% yield (Scheme 11a).[20] The two "inner" bromides of hexa-brominated QDI **55** also exhibited high reactivity in Stille coupling reaction. Therefore the hexa-thiophenyl substituted QDI was obtained which could further be cyclodehydrogenated to form the hexa-thiophene annulated QDI **57**.[31] Direct fusion of thiophene rings and rylene core (i.e. **54** and **57**) drastically influenced their orbital energy levels and thus optical and electronic properties when compared to their corresponding parent TDI and QDI precursors. For example, these thiophene-annulated RDIs have high potential of being applied in ambipolar semiconductors. Also, the synthesis of dibenzopentarylene diimide **60** was feasible and might be considered as the core expansion of 5DI (**4**).[12b] Like in the case of bisanthracene diimide **49**, the additional two phenyl rings of **60** are fused at the naphthalene units of rylene, however not in the *bay*-region. **60** was synthesized from 5,11-dibromotetracene **58** and PMI-boronic ester **13'** with two substitutions at the 1,6-*bay*-position to retain high solubility of the target molecule. Suzuki coupling of **58** and **13'** afforded the bis-PMI-tetracene triads **59**. In contrast to the synthesis of **52**, **54** and **57** in which the final cyclodehydrogenation of eight or even twelve protons went smoothly in one step, the final cyclization of **59** under Scholl conditions using $FeCl_3$/nitromethane in CH_2Cl_2 gave only a half-fused intermediate. Therefore, a second base-promoted reaction with K_2CO_3/ethanolamine was necessary in order to generate the target dibenzopentarylene diimide **60** (Scheme 11b). Thus, choosing proper condition for the key reaction of ring cyclization in higher rylene diimide is of primary importance. Due to the electronically deficient precursors (usually bearing imide moieties), the commonly used Lewis acid-induced oxidative cyclodehydrogenation method proved to be unfavorable and led to undesirable dealkylation. Most of the reported ring cyclization reactions in rylene diimides synthesis involve base-induced ring-formation. Typical conditions include molten KOH, K_2CO_3 in ethanolamine, t-BuOK/DBN in diglyme, etc. When the desired C-H bonds for ring cyclization is far from the imide groups, the popular used system of $FeCl_3/CH_3NO_2$ can also be considered (e.g. Scheme 3, Scheme 11b). In some special cases, a combination of several different conditions was necessary.

2.1.4 Five membered ring annulation at the bay positions

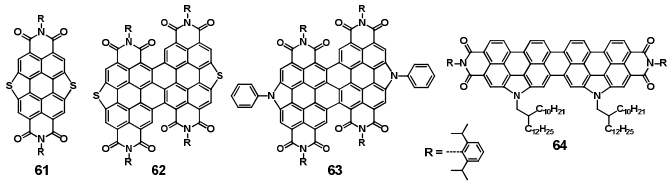

Scheme 12. Reported five membered heterocyclic annulated RDIs **61**-**64**.

Apart from the aforementioned six-membered ring annulation of additional benzene rings and heterocycles (**51**-**54**, **56**-**57**) at the *bay*-positions, several interesting examples of five-membered ring annulation (**61**-**64**) of heteroatoms (i.e. S or N) were reported as well, as shown in Scheme 12. The S-heterocyclic annulated PDI **61** was prepared in a one-step $Pd(PPh_3)_4$-catalyzed Stille-type reaction of readily available 1,6,7,12-tetrachloro-PDI **34a** with $Bu_3SnSSnBu_3$ in refluxing toluene in 72% yield, appearing as an orange-yellow solid.[34] Furthermore, an "upgraded" version of S-heterocyclic annulated diPDI (S-diPDI) **62** was obtained as blue-black solid in 68% yield under the same reaction conditions with tetrachloro-diPDI **35a-1** as starting material.[35] Furthermore, $Pd(OAc)_2$-catalyzed Buchwald-Hartwig reaction of **35a**-**1** with aniline afforded the N-heterocyclic annulated diPDI **63** as green-black solids in a 51% yield.[35] Similar to the core expanded CDI, the five-membered ring annulated S-PDI **61** (λ_{max} = 480 nm), S-diPDI **62** (λ_{max} =633 nm), and N-diPDI **63** (λ_{max} = 670 nm) showed hypsochromic shifts of 47, 51, and 14 nm in respect to their non-annulated counterparts respectively. In parallel to these works, a five-membered N-heterocyclic ring annulated QDI **64** was developed by Wu's group.[36] However, this ladder-type bis-N-annulated QDI **64** was not directly synthesized from QDI but through a multi-step synthesis from the N-annulated perylene. It is noteworthy to mention that compound **64** exhibited absorption in the NIR region and emitted strong fluorescence with quantum yield up to 55% in dichloromethane which is approximately ten times higher than that of the parent QDI (ca. 5%). The higher fluorescence quantum yield of **64** could account for the introduction of two bulk 2,6-diisopropylphenyl groups which inhibit the aggregation, the two dove-tailed alkyl chains, and the calculated bent geometric structure due to the two five-membered ring annulation. Such a high quantum yield is remarkable considering that many other NIR absorbing dyes usually exhibit low fluorescence quantum yield or are even non-emissive.

2.2 Push-pull effect and quinoidal charge delocalization

Higher RDIs showing significant bathochromic shift to the NIR region are, besides from extension of π-conjugation by a multi-step synthesis, accessible by several other strategies as well: i) incorporation of donor and acceptor substituents; ii) formation of quinoidal structures; iii) covalent linkage of multiple RDIs. Those strategies will briefly be described by means of typical examples. As already briefly discussed above, the introduction of substituents such as phenoxy or alkylamino groups to the *bay*-positions of perylene imides has been widely applied in rylene chemistry. These substituents not only improve their solubility and processability but also allow control over their energy levels.[37] Substitution with phenoxy arms in the *bay*-positions is one of the most popular ways to increase the solubility of rylene imide dyes.[38] Moreover, the electron donating nature of phenoxy groups also enhance the intramolecular charge transfer effect and thus induce an additional bathochromic shift. Substitution in the bay area with large phenoxy-based polyphenylene dendrons not only improve the solubility in organic solvents but has also been found to protect the core chromophore from oxygen or radicals.[39] The substitution of piperidyl groups in the *bay*-positions resulted in

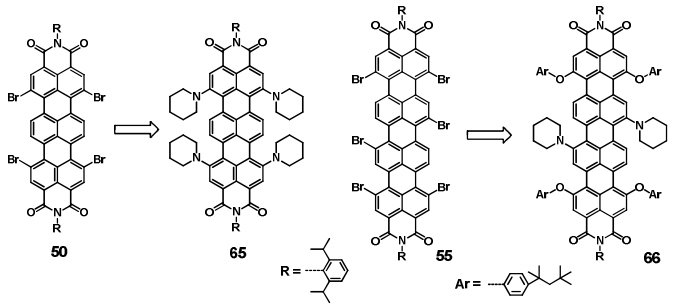

Scheme 13. Piperidyl substitution of TDI and QDI at *bay*-positions.

a more pronounced push-pull effect compared with phenoxylation, and therefore a bathochromic shift of 170 nm for **65** (λ_{max} = 819 nm)[10b-c] and 148 nm for **66** (λ_{max} = 910 nm),[10b-c] compared with their counterparts without piperidyl substitution (Scheme 13), respectively.

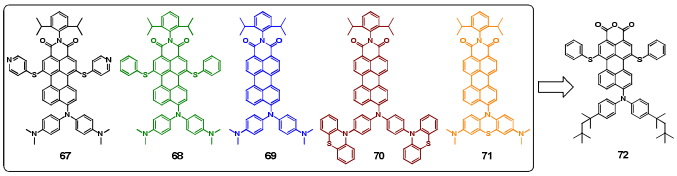

Scheme 14. Chemical structures of "push-pull" PMIs **67**-**71** and a related best perylene imide based sensitizer **72** for DSSCs.

A more pronounced push-pull effect was observed by introduction of donor and acceptor substituents to the opposite *peri*-positions of the perylene core. The "push-pull" family of perylenes (**67**-**71**) was generated by three-step reactions using the carboxylic diimide group of PMIs as electron acceptor and functionalizing the 1-, 6-, and 9-positions selectively with different donors (Scheme 14).[40] These dyes exhibit a rainbow of colors as well as tunable properties. The *peri*-substituents coarsely tune both the spectroscopic and electrochemical properties of PMIs, whereas the bay substituents allow additional fine tuning. Thus, their absorption are readily shifted throughout the entire visible and even into parts of the NIR region by changing the donor and acceptor strengths as well as the position in which the substituents are attached to the scaffold of the perylenes. Moreover, molecular orbital calculations and optical measurements indicated occurrence of intramolecular charge transfer when the perylene core is functionalized with a donor and an acceptor substituent in the opposite *peri*-positions.[39] Based on these results, a highly efficient perylene sensitizer **72** was designed by careful selection of the appropriate substituents in the *bay*- and *peri*-positions. The resulting PMIs were modified with anhydride groups for their use in dye sensitized solar cells (DSSCs). Finally, saponification gave dicarboxylic acid groups, which were able to bind TiO_2 surface. When included in DSSCs, the perylene monoanhydride (PMA) **72** revealed an incident monochromatic photon-to-current conversion efficiency of 87% as well as a power conversion efficiency of 6.8% under standard AM 1.5 solar conditions. The fine-tuning of the substituents provided a powerful way to generate new perylene sensitizers with stronger intramolecular charge transfer (ICT), more suitable HOMO or LUMO energies, and more desired light absorption properties for solar energy conversion.

Besides the introduction of stronger donors to the 9-position of perylene, donor functionalization of both *peri*-positions (9,10-position) provides another promising way of enhancing the push-pull character, compared to the conventional 9-donor-substituted PMIs.[40] Direct bromination at the 9,10-positions of PMI is always accompanied by the side bromination of one or

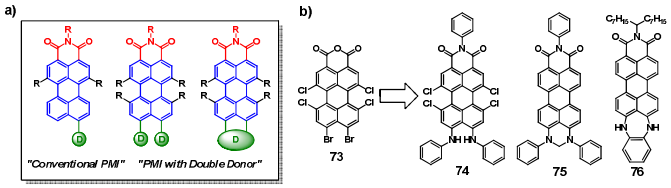

Scheme 15. a) The structural comparison of conventional and double donor substituted "push-pull" PMI. Adapted with permission from Ref. [42], Copyright 2012, American Chemical Society; b) Key intermediate and selected examples of double donor substituted PMI.

even both *bay*-positions (1,6-position).[41] Additionally, the subsequent reactions of the brominated PMI normally take place in the *bay*-positions. A facile synthetic method toward solely 9,10-functionalized PMIs (Scheme 15) was described by our group.[42] For simultaneous introduction of two donor groups to the *peri*-positions of the PMI skeleton, we carried out a selective Hunsdiecker reaction using inexpensive reagents like sodium hydroxide, acetic acid, and bromine. To ensure sufficient solubility of all intermediates, the commercially available tetrachloroperylene dicarboxylic acid anhydride (PDA) was selected as the starting material. Upon sequentially adding aqueous sodium hydroxide, acetic acid, and bromine to tetrachloro-PDA, the key building block: 9,10-dibromo-dicarboxylic acid monoanhydride (**73**) was obtained in 85% yield. A twofold aromatic amination and imidation with aniline in a one-pot reaction gave compound **74** in a 70% yield. Subsequently, a methylene bridge was introduced between the two amine donors and the four chlorine substituents were cleaved yielding **75**. Similarly, another double donor PMI **76** was obtained by imidation of **73** with 8-pentadecanamine, followed by further amination with 1,2-diaminobenzene, and final dechlorination using potassium hydroxide in ethylene glycol. All double donor PMIs with 9,10-functionalization exhibit broad absorption bands, typical for "push-pull" type molecules. For example, **75** displayed a similar absorption spectrum as the unsubstituted PMIs having two maxima at 626 and 660 nm. In comparison to the unsubstituted PMI **11**, **75** exhibits a similarly shaped absorption band, however, with a large bathochromic shift (ca.150 nm) and a strongly enhanced extinction coefficient indicating a synergistic pushing effect by the two symmetric donor groups in the 9,10- positions. The fluorescence of compounds **75** and **76** is almost quenched, which indicates an efficient photoinduced intramolecular charge transfer (CT) takes place in both compounds. Owing to the broad absorption bands in the Vis-NIR region and additionally strong CT behavior, **75** and **76** are outstanding candidates for application in photovoltaics, especially in DSSCs.

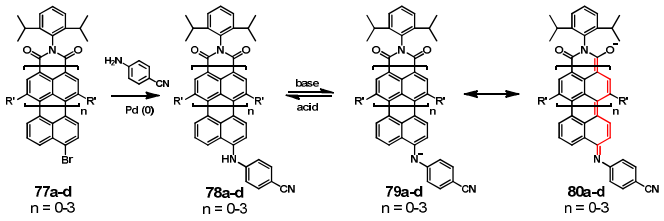

Scheme 16. Synthesis of quinoidal ryleneimide dyes **80**.

Another novel approach towards higher RDIs with NIR absorption involved protonation and subsequent quinoidal charge delocalization of RDIs with amino-substitution at the

peri-positions using a strong base. Naphthalene, perylene, terrylene and quaterrylene monoimides **77** were reacted with 4-cyanoaniline in order to give the homologue series **78** (Scheme 16). Upon addition of a base and subsequent removal of the amino proton, the negative charge is delocalized at the imide oxygen resulting in a quinoidal structure (Scheme 16, red color).[43] This type of conjugation is responsible for vast bathochromic shift increases with increasing molecular size, resulting in a giant bathochromic shift of 435 nm for the quaterrylene derivative **79d**. Amination of imides **77a-d** introduced a "push–pull" effect to the molecules resulting in bathochromic shifts of 16–91 nm. Evidently, the "push–pull" effect decreased from dye **78a** to **78d** due to the increasing size of the π-system. Most interestingly, dyes **80a**–**d** exhibit significant bathochromic shifts (135-435 nm), compared to the absorptions of **78a-d**, due to the quinoidal charge delocalization. The quinoidization of dyes **78a**–**78c** also led to a significant increase of their extinction coefficients.

2.3 Multichromophores

Owing to a broad overlap of the PDI emission spectrum with the TDI absorption spectrum, a combination of these two dyes is desirable to create bi- and multichromophoric systems which can be studied regarding energy and electron transfer between the two. The distance between chromophores can be easily varied by the length of the spacer group between PDI and TDI.[44] Another approach regarding the multichromophore design involves 3D-shaped polyphenylene dendrimers, where highly twisted pentaphenyl units form a photochemically inert and shape-persistent dendritic scaffold around the energy acceptor chromophore, which was pre-decorated with donor chromophores on the surface. This variation is a useful way to enlarge the spectral range of the dyes for photovoltaic applications.[45] These multichromophores absorb over the whole range of the visible spectrum but only show an emission from the central-chromophore TDI due to efficient energy transfer.[46]

Together with the group of Basché, we reported experiments towards single-pair electronic excitation energy transfer (EET) in a dyad, built from PDI as donor, TDI as acceptor and a *p*-terphenyl spacer (dyad **81**, Figure 3) as bridging group in 2004.[47] Since then, several further single molecular as well as theoretical studies on this compound have been carried out to

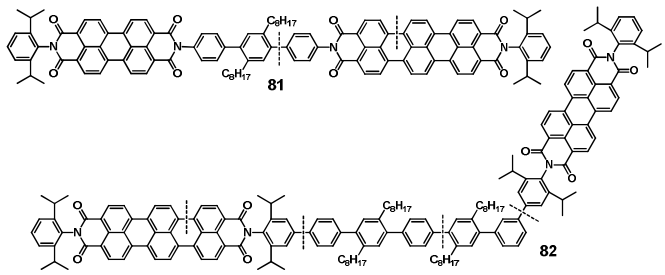

Figure 3. Molecular structures and retrosynthesis of the linear dyad **81** and kinked dyad **82** with PDI and TDI.

understand the prevailing energy transfer (EET) process and evaluate the limits of the Förster theory.[48] In this section, we summarize the synthesis of multichromophores including dyads, triads, dendritic and star-shaped systems, with an emphasis on the structural design. The key reactions involved imidation, Suzuki coupling, and cyclization of biaryl intermediates to ribbon-type arenes. Among the many possible approaches toward the synthesis of dyad **81**, we chose an optimized balance between solubility and reactivity of the building blocks for each reaction.[49] Both the key steps of synthesis of dyad **81** and **82** (Figure 3) involve Suzuki coupling of the asymmetric functionalized PDI and TDI precursor **14** (Scheme 1).

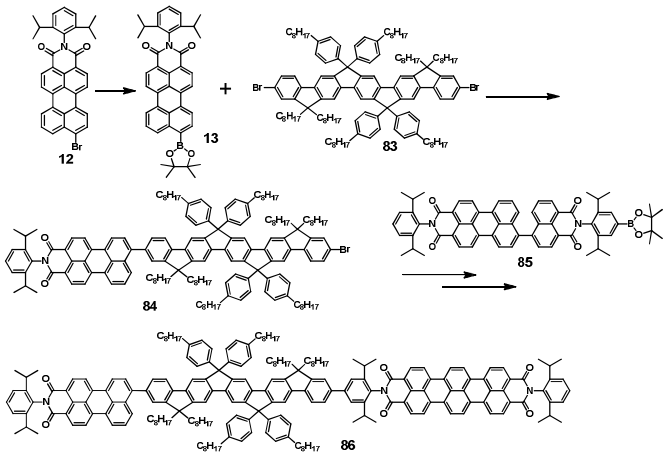

Scheme 17. Synthesis of model dyad PMI-*p*Ph-Ph-TDI **86**.

A dyad **86** was designed with a PMI donor connected to a TDI acceptor through a ladder-type pentaphenylene (pPh) spacer (**83**)[50] to enhance the bridge-mediated contributions to electron coupling in the electronic energy transfer process between the donor and the spacer in this dyad system. The synthesis of the rigid ladder-type pPh spacer **83** was described elsewhere.[51] As discussed above, the facile synthesis of the PMI-boronic ester **13** and of the boronic ester **85** paved the way for the target dyad **86**. As illustrated in Scheme 17, selective one-fold Suzuki coupling of spacer **83** with **13** afforded the PMI-pPh-Br **84** which was subsequently coupled with **85** by Suzuki coupling reaction. This resulted precursor was further cyclized to provide the target dyad **86**.

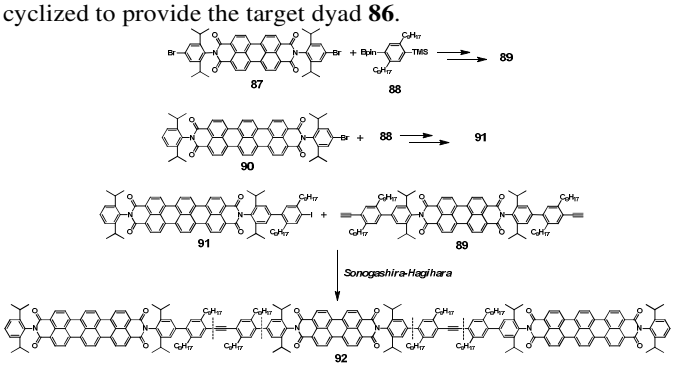

Scheme 18. Synthesis of TDI-PDI-TDI (A-D-A type) triad **92**.

Besides the dyads, we also reported a linear triad **92** (Scheme 18) with PDI as donor and two TDIs as acceptors.[52] The synthesis of this acceptor-donor-acceptor (A-D-A) multichromophore was accomplished by the Sonogashira coupling of an asymmetric TDI **91** and a bifunctional PDI **89**. At first, the bifunctionalized dibromophenyl-PDI **87** was synthesized by imidation of perylene-3,4,9,10-tetracarboxylic acid dianhydride (PDA) and 4-bromo-2,6-diisopropylaniline. After Suzuki coupling, halogenation and Sonogashira coupling, the 5-(2-ethynyl-1,4-dioctyl) phenyl end-caped PDI **89** was obtained from **87** and **88**. The asymmetrically functionalized TDI **90** was synthesized by cyclization of its open form **14** (Scheme 1). The asymmetric TDI **91** was obtained by using Suzuki coupling with 2,5-dioctyl-4-(trimethylsilyl)phenyl) pinacolate boronic ester **88**, followed by halogenation with ICl leading to conversion of the trimethylsilyl group into the

corresponding iodide **91**. Further Sonogashira coupling of **89** and **91** afforded the triad **92** (Scheme 18).

Dendrimers are a class of macromolecules having precisely controlled branched structures and consist of a core, a branched scaffold, and an external surface.[53] Dendrimers have been shown to possess unique physical and chemical properties which differ significantly from that of their linear oligomer and polymer counterparts.[54] The use of a fluorescent chromophore as core enables the application of fluorescence spectroscopy to study structural aspects and conformational mobility of dendrimers in solution.[55] Moreover, the dendritic shell with its specific nanometer-sized environment isolates the chromophores, making them interesting for single-molecule spectroscopy (SMS) studies. The synthesis of dendrimers having fluorescent chromophores attached to the rim displays an efficient way toward well-defined numbers of chromophores in a confined molecular size.[56] Another essential advantage of the dendrimer-based design of multichromophores is complete avoidance of dye aggregation. Here we present two exemplary dendrimers to illustrate how TDIs and PMIs are functionalized through multichromophoric dendrimer synthesis.

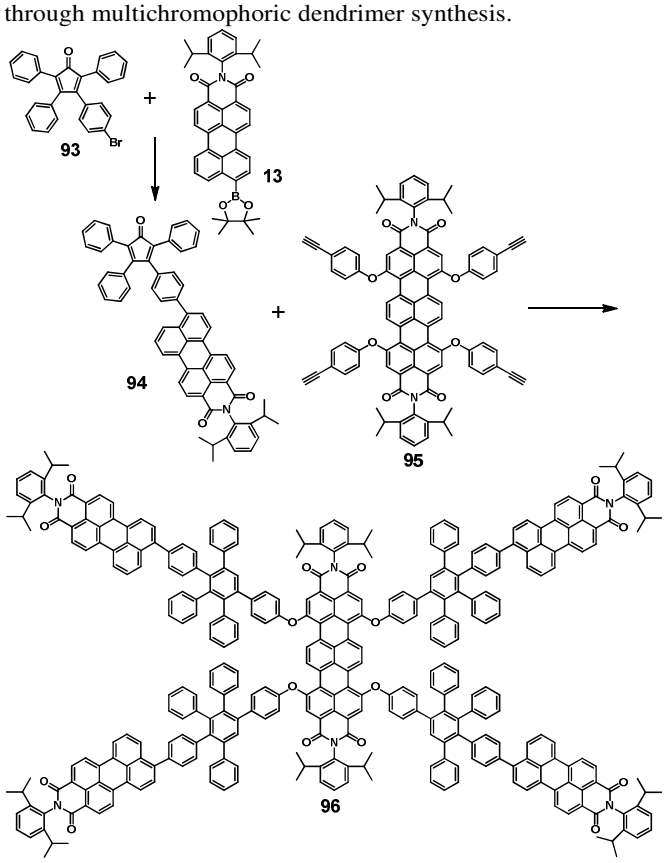

Scheme 19. Synthesis of 4PMI-TDI based dendrimer multichromophore **96**.

The 4PMI-TDI based dendrimer **96** [57] consists of a terrylene diimide (TDI) unit acting as energy acceptor in the core and four perylene monoimide (PMI) units serving as energy donors in the periphery. We chose these chromophores (TDI and PMI) because of their photostability, high extinction coefficients at convenient absorption wavelengths (λ_{max} = 495 nm and λ_{max} = 673 nm for PMI and TDI, respectively), high fluorescence quantum yields, and good overlap between the emission of PMI and the absorption of TDI. This permits efficient intramolecular Förster energy transfer. The synthetic approach is based on the Diels-Alder cycloaddition of a tetraphenylcyclopentadienone (Cp) system containing the dye molecule (PMI) with ethynyl-functionalized TDI. At first, the monobromo-Cp **93** was coupled with the PMI-boronic ester **13** to generate the PMI-containing Cp **94**. A fourfold Diels-Alder reaction of **94** with a tetra-ethynyl functionalized TDI **95** afforded the target multichromophoric dendrimer **96** in 92% yield (Scheme 19). The number of bromo groups in compound **93** determines the final number of PMIs in the dendrimer. Moreover, various pairs of chromophores at the rim and the core of the dendrimer could thus be established with this strategy.

In Scheme 20, another example of a first-generation polyphenylene dendrimer (**98**) having a rigid tetrahedral core and four PMI chromophores at the rim is shown.[58] Target compound **98** was synthesized by the efficient Diels-Alder reaction of tetrakis(4-ethynylphenyl)methane (**97**) with the PMI decorated cyclopentadienenone **94** in 90% yield.[59] In order to study the energy transfer in such multichromophoric systems systematically, the numbers of PMI chromophores were varied from one to four along the branches of the dendrimer in the direction of the corners of a tetrahedron.[59-60] For asymmetric functionalization of the periphery of polyphenylene dendrimer,

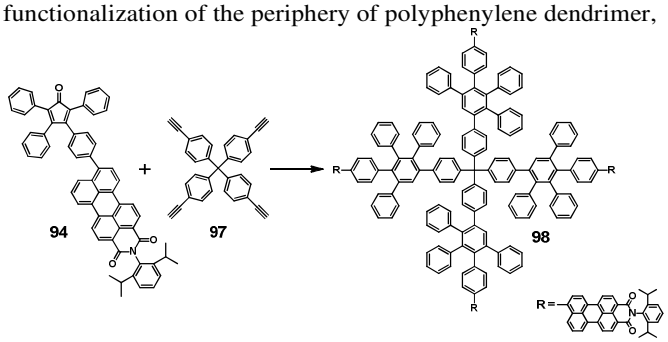

Scheme 20. Synthesis of model dyad G1-4PMI **98.**

a stepwise Diels-Alder reaction of the triisopropylsilyl (TIPS) protected tetraphenyl methane and Cp with or without PMI branches were used.

The last example of the multichoromophore system summarized in this feature article is the star-shaped PMI-substituted hexa-*peri*-hexabenzocoronene (HBC) **100**, which was designed as model compound for intermolecular energy and electron transfer studies owing to its D_{6h} symmetry, electronic as well as self-assembling properties.[61] For the generation of multichoromophore (HBC-6PMI) **100**, six PMI chromophores were attached to the HBC *via* a 3'-dodecyl-4',5',6'-triphenyl-1,1':2',1''-terphenyl spacer unit (in green color, Scheme 21). HBC-6PMI **100** was finally obtained by Diels-Alder reaction of hexa-[4-(tetradec-1-yn-1-yl)phenyl]-HBC **99**[25] and well-established building block **94**, a PMI decorated Cp, in diphenyl ether at 250 °C and in 58% yield. Indeed, electronic excitation of the HBC core of this molecule resulted in efficient energy transfer to the PMI shell.[62-63]

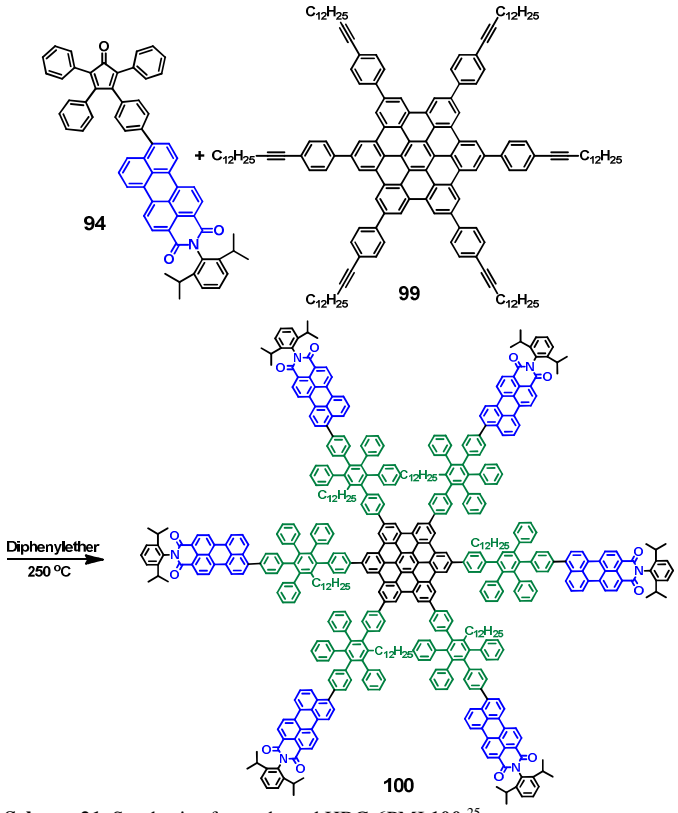

Scheme 21. Synthesis of star-shaped HBC-6PMI **100**.[25]

2.4 Combination of different dyes

There is increasing attention on hybrid chromophores obtained by the combination of different well-known and high performance dyes. Typical examples include fusion of porphyrin and anthracenes,[64] annulation of anthracene to 4-bora-3*a*,4*a*-diaza-*s*-indacene (BODIPY),[65] porphyrin-fused BODIPY,[66] and diketopyrrolopyrrole (DPP)-conjugated BODIPY.[67] Concerning rylene dyes, there are also some reports of fusing rylene imides with other well-known chromophoric systems like porphyrin and zethrene. Here we show two examples to illustrate how it works and how efficient it is. One of the most utilized pathways to obtain such ladder-type fused hybrid chromophores is the intramolecular ring-closure reaction of the singly linked dyads, which are usually prepared by Pd-catalyzed cross-coupling reactions between aromatic building blocks having appropriate geometric and electronic structure. Thus, the precursor PMI-porphyrin dyad was synthesized by Suzuki coupling of PMI boronic ester **13** and porphyrin monobromide followed by metalation with $Ni(acac)_2$. The subsequent ring closure of the PMI-porphyrin dyad with excess of $FeCl_3$ under refluxing dichloromethane generated doubly linked PMI-porphyrin **101** in 38% yield as a purple solid (Figure 4). Interestingly, an unexpected triply linked PMI-porphyrin (**102**) was also isolated in 25% yield as a green solid. The doubly (*peri*-meso; *peri*-β) linkage between the PMI and porphyrin moieties in **101** lead to an intensive NIR absorption maximum at 803 nm. Comparing **101** to the triply linked compound **102** having an additional meta-β' linkage, **102** has a further bathochromic shift of 94 nm. The electron-withdrawing dicarboxylic imide groups in **101** and **102** significantly lower their HOMO energy levels. Therefore they exhibit improved long-term stability against air and light, compared to their former *N*-annulated perylene-fused porphyrins.[68] More importantly, such push-pull structures facilitate a fast electron injection from the excited state of the dye to the conduction band to TiO_2 in DSSCs. Accordingly, two perylene anhydride fused porphyrins were synthesized by the same group via saponification of the imide groups in the presence of a strong base. Also, their performance as NIR sensitizers for DSSCs was tested.[69] Both compounds exhibited broad monochromatic photo-to-current conversion efficiency spectra covering the whole visible spectral region and even part of the NIR region up to 1000 nm, which is very impressive for the ruthenium-free sensitizers in DSSCs.

Zethrene is a series of aromatic hydrocarbons where two phenalenyl moieties are fused "head to head", thus bearing a unique Z-shaped molecular skeleton. Based on theoretical predictions, the parent zethrene possess a singlet biradical

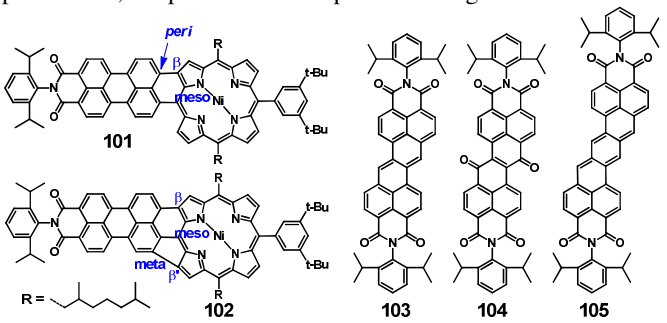

Figure 4. Molecular structures of porphyrin fused PMI **101**-**102** and zethrene diimides **103**-**105**.

character[70] and therefore is a promising candidate for non-linear optics, ambipolar FETs and spintronics.[71] Unfortunately, most of the zethrene derivatives reported so far exhibited typical closed-shell features and were air-sensitive. In order to overcome these drawbacks, Wu and coworkers[72] reported the electron-withdrawing dicarboxylic imide group substituted zethrene derivatives **103** and **105** (Figure 4). This substitution not only stabilized the highly reactive zethrene by lowering its HOMO energy level, but also led to a pronounced red-shift of the absorption and emission. **103** was synthesized by Stille cross coupling reaction of 4,6-dibromo-NMI with bis(tributylstannyl)acetylene and subsequent *in situ* transannular cyclization reaction. The larger heptazethrene diimide **105** was synthesized by a similar intramolecular transannular cyclization of its diacetylene precursor. Interestingly, differently from zethrene itself, diimide **103** still owns a typical closed-shell feature, while heptazethrene diimide **105** possesses an open-shell biradical character as demonstrated both by the ^{1}H NMR measurements and calculations. Further functionalization of the zethrene diimide **103** at the 7,14-positions using N-bromosuccinimide (NBS) in DMF generated the oxidized quinone derivative **104** rather than a bromination product which is related to the central butadiene character in the zethrene unit of **103**.

Overall these hybrid chromophore concepts provided an efficient way of accessing higher RDIs dyes which combine properties of each chromophore building block. To achieve a high performance of these dyes in real application, the processing techniques, in particular the supramolecular organization, are equally important. In the following section, we are going to describe the investigation on rylene diimides regarding self-assembly and the relationship between molecular ordering and device performance.

3. Self-assembly

The spontaneous self-assembly of small molecules to form soft functional material having ordered supramolecular structures in nano-, meso-, or macro-scopic scales is gaining interest of chemists, biologists and material scientists. Rylene diimides, typically PDI and its higher homologues, are promising n-type semiconductors for application in organic electronic devices due to their strong electron affinities and high electron mobility. To achieve better device performance of such materials, the processing techniques of orienting these molecules in highly ordered spatial arrangement is of primary importance. Thus, the studies on supramolecular assembly of such rylene imide dyes and on understanding the relationship of mesoscopic ordering and properties are essential. Würthner and coworkers did a lot of nice work concerning supramolecular self-assembly of PDI derivatives and several excellent reviews from the same group were published.[1a] Therefore we are solely focusing on the recent self-assembly studies on the higher RDI derivatives.

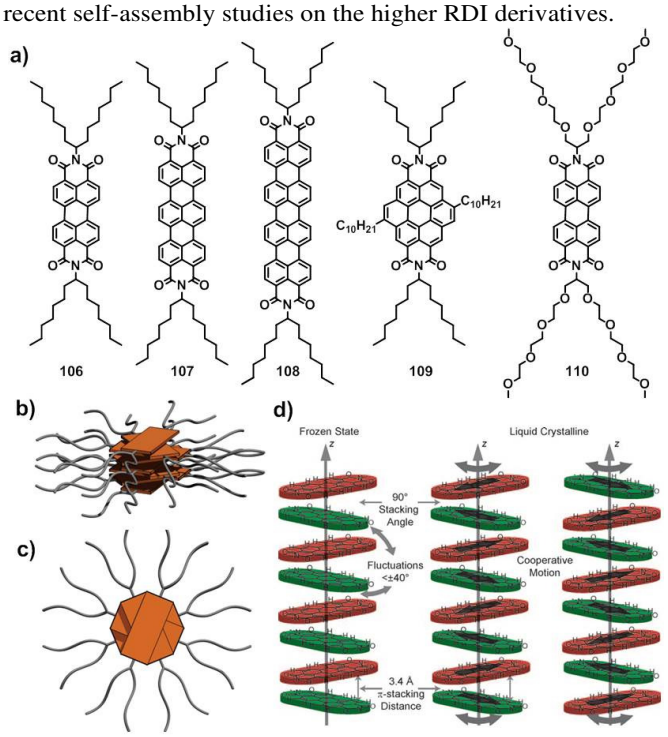

Figure 5. a) Molecular structures of RDIs **106**-**110**; b) side and c) top views of packing of **106**-**108** with branched alkyl chains, Reproduced with permission from Ref. [11b], Copyright 2006, American Chemical Society; d) organization and molecular dynamics of triethyleneglycol substituted **110**. Reproduced with permission from Ref. [73], Copyright 2009, Wiley-VCH.

Our group reported the systematic investigation on a homologous series of branched heptyloctyl chains substituted diimides, namely PDI **106**, TDI **107**, QDI **108** and CDI **109** (Figure 5a).[11b] These diimide dyes exhibit absorption maxima in the range of 430-760 nm covering the whole visible light region with high extinction coefficients and show high thermal stabilities tolerating temperatures up to 450 °C. Interestingly, systematic structural analysis of these four dyes (**106**-**109**) by X-ray diffraction analysis and solid-state NMR studies confirmed an identical molecular twist of 45°, independent from their core size (Figure 5b-5c). For example, the structural analysis of **106** was done by calculating the X-ray pattern based on molecular dynamic simulation in which the discs equilibrated into helical structure having an intermolecular rotation angle of 45°. On the contrary, solid-state NMR studies on **106** suggested a little broader range for the rotation angle (30-45°) which was mainly assigned to the out of plane rotation of the bulky alkyl side chains toward the aromatic core. When deposited on substrate (e.g. Si wafer), RDI **106**-**108** formed large and highly ordered domains with an "edge-on" orientation, while the CDI **109** self-organized in a "face-on" manner leading to a homeotropic phase.

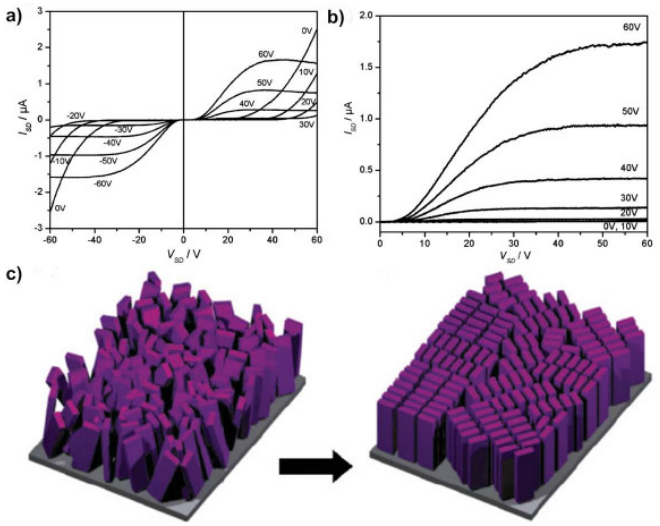

Figure 6. Output characteristics of FET devices based on QDI **108**: a) before and b) after thermally annealing the device at 100°C for 1h. c) Schematic illustration of the supramolecular organization of QDI **108** before and after annealing.[74] Reproduced with permission from Ref. [74], Copyright 2008, Wiley-VCH.

Although the packing mode of these rylene diimides was independent of their core size, the side chains substituted at the two imide N-termini seemed to play a more important role. For example, the replacement of the hydrophobic alkyl side chains at the PDI core with hydrophilic triethylene glycol (as in **110**) not only led to a more apparent liquid crystalline (LC) behavior with distinct molecular dynamics, but also changed the lateral rotation between neighboring molecules from 45° to a perpendicular packing of 90°.[73] Solid-state NMR results were in good agreement with the X-ray data revealing different axial motions for **110** in its two phases (i.e. frozen state and LC phase, Figure 5d). Not only the intrinsic chemical nature of molecules determined their device performance, but also the processing conditions made a big difference. Taking QDI **108** as an example, a bottom gold contact, bottom gate field-effect transistor (FET), was fabricated by drop-casting a 1,2-dichlorobenzene solution of QDI **108** on a silicon substrate.[74] This thin film FET device exhibited ambipolarity for both hole and electron transport (Figure 6a). Surprisingly, the hole conduction disappeared after thermal treatment at 100 °C for 1 h (Figure 6b). This absence of *p*-type behavior was induced by morphology changes upon thermal annealing, as demonstrated by X-ray diffraction studies (Figure 6c-d). Although the control of the morphology is an important parameter in electronic devices, it seems that, in this case, the gain in orientation had no favorable impact on the hole conductivity.

The combination of HBC as donor and PDI as acceptor material has been applied successfully in hetereojunction photovoltaics.[75] Accordingly, a *C6* symmetric hexa-PDI-substituted HBC **111** and a control compound PDI-HBC dyad **112** were designed to investigate the effect of molecular

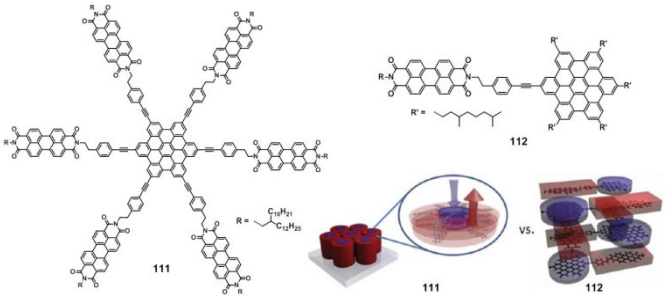

Figure 7. Molecular structures of HBC-PDI dyads **111**-**112** and the columnar stacks of **111** and interdigitating stacks of **112**. Modified with permission from Ref. [76], Copyright 2012, American Chemical Society.

geometry on their assembly behavior as well as charge transport properties (Figure 7).[76] The peripheral alkyl-chains and the bridge between donor (HBC) and acceptor (PDI) are important for the properties of the molecule. To control the morphology at the nano-scale, the PDI was covalently bonded by an ethynyl linker to the HBC core resulting in a new kind of dyads with an intercolumnar phase separation between donor/acceptor stacks. Moreover, the ethynyl bridge interrupts conjugation between donor and acceptor resulting in higher flexibility and therefore solubility. Furthermore, branched alkyl chains were also introduced into the periphery to enhance the solubility of PDI and of the target compound. This starburst molecule still formed discotic mesophases. It is extraordinary intriguing to study the photophysical properties of the single molecule as well as of aggregates and the mesophase. Depending on the symmetry of the dyads, a columnar stacking was observed for the *C6* symmetric dyad **111** while an interdigitating network with alternating HBC and PDI moieties was formed with dyad **112**. For dyad **111**, an efficient intramolecular Förster-type resonance energy transfer from the HBC unit to the PDI part was observed. In contrast, efficient electron transfer was observed in the alternating stacks of HBC and PDI units of the linear dyad **112**. Interestingly, the star-shaped dyad **111** provided potential transport channels for both holes and electrons along the columns and also no electronic interactions between the donor and acceptor were found due to the long distance (ca. 2.1 nm). These independent transport channels represented a type of "coaxial cable" which is required in electronic devices.

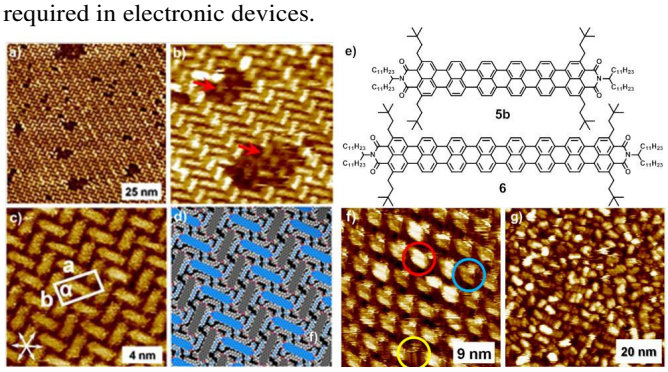

Figure 8. Self-assembled networks of HDI and ODI. a) Large scale STM image showing herringbone type arrangement of HDI (C_{HDI} = 5.2 × 10^{-7} M). b) STM image (27.4 × 27.4 nm^2) showing the presence of lower layer (red arrows) at a defect site. c) Enlarged STM image showing the molecular arrangement in detail. Unit cell parameters are: a = 4.67 ± 0.09 nm, b = 2.41 ± 0.04 nm and α = 89.7 ± 1.5°.The white arrows in the lower left corner indicate the symmetry axes of HOPG lattice. d) Molecular model of the herringbone pattern of HDI. Alternate rows are colored differently for the sake of clarity. e) Molecular structures of HDI **5b** and ODI **6**. f) Multilayer formation of HDI g) Disordered multilayers of ODI. Adapted with permission from Ref. [17], Copyright 2013, Wiley-VCH.

Although higher RDIs have been reported for almost twenty years, the self-organization on liquid-solid interfaces and real visualization of the single molecule by scanning tunneling microscopy (STM) has just proved to be successful recently.[17] Here, we take the two longest HDI and ODI as examples to illustrate their unique assembly behavior in contrast to other disc shaped molecules. When adsorbed from relatively dilute (5.2 × 10^{-7} M) 1,2,4-trichlorobenzene (TCB) solution, HDI formed large domains of herringbone type arrangement (Figure 8a). The molecular layer revealed the presence of numerous defects which are rather unusual for self-assembly at the liquid-solid interface which is known to favor formation of defect-free monolayers.[77] Further inspection of the STM images disclosed that, despite of the low surface coverage at this concentration, the molecular layer actually consisted of two layers of molecules adsorbed on top of each other and the defects were only present in the second layer (Figure 8b). A high-resolution STM image revealed that the HDI molecules are closely packed in a "face-on" orientation on the HOPG surface (Figure 8c). The rectangular unit cell of HDI consists of two molecules. A molecular model based on unit cell parameters (Figure 8d) indicated that intermolecular interactions are not driven by the π-π interactions between the molecules and the graphite surface.[78] In fact, at concentrations higher than 1.7 × 10^{-5} M, HDI forms hierarchical multilayers at the TCB/HOPG interface and up to three layers could be identified (Figure 8f). The formation of such robust and stable multilayers at the liquid-solid interface is unprecedented. In contrast to the extended networks observed for HDI, self-assembly of ODI at the TCB/HOPG interface leads to formation of disordered multilayers (Figure 8g). Such multilayers were observed for solution concentration down to 5.0 × 10^{-6} M. Further decreasing of the concentration did not lead to adsorption of ODI on the HOPG surface. We believe that disordered aggregates observed for ODI are reminiscent of their strong pre-assembly.

4. Applications

4.1 Organic semiconductors in OFETs and OPVs

Due to their outstanding properties, rylene dyes are not only suited for single molecular spectroscopy studies, but are also applied in the field of organic semiconductors in electronic devices such as FETs,[79] photovoltaic cells[80] or LEDs. The electron-withdrawing imide structures of *N*,*N*-alkyl- PDI are responsible for their n-type character[81] in thin-film transistors.[82] Furthermore, PDI where the *bay*–positions were substituted with electron withdrawing cyano groups and the imides positions were substituted by perfluoroalkyl chains , the highest mobility of up to 6 cm^2/Vs was achieved.[83] As for the organic photovoltaics (OPVs), the use of perylene dyes for organic solar cells can be traced back to the first organic photovoltaic cell fabricated by Tang, where phthalocyanine and perylene diimides derivatives were used as active materials with a reasonable power conversion efficiency of up to 1%.[84] The tunable solubility, controlled optical and electrochemical properties of perylene imides dyes upon functionalization made them a promising candidate for various organic solar cells. Many studies have been devoted to the improvement of photovoltaic performance by applying different derivatives of perylene imides and metal phthalocyanines. Bazan and coworkers reported one of the best efficiency (3%) so far for the bulk heterojunction solar cell using PDI as a non-fullerene

acceptor.[85] The relatively poor performances of RDIs as acceptors in solar cells are probably derived from their strong tendency to crystallize resulting in poor phase separation between the donor and acceptor materials.

Another significant step toward organic thin film photovoltaic devices was achieved by a combination of the liquid-crystalline hexa-*peri*-hexabenzocoronene (HBC) and a PDI having branched alkyl chains.[75a] By the use of a blending technique, these materials were allowed to self-assemble into a two-phase photovoltaic material which showed an extraordinary performance. For such photovoltaic cells, a quantum efficiency (the ratio of light absorbed to electrical energy produced) of 34% was achieved using light with a wavelength of 490 nm. In order to increase the efficiency of organic solar cells and to cover light also in the NIR region, perylene-, terrylene-, and quaterrylene-tetracarboxdiimide derivatives with branched alkyl chains were synthesized. They exhibit a high degree of order in bulk since they form discotic columnar phases with large and highly ordered domains ensuring undisturbed percolation pathway for charge carriers between electrodes in photovoltaic devices. A high degree of order was also found in blends of these materials with HBC.[86] Besides using HBC as *p*-type semiconductor, efficient photovoltaic cells have been obtained using PDIs blended with polycarbazole.[87] Another promising approach to obtain organic photovoltaic materials consisted of covalent coupling of PDI with oligothiophenes.[88] Perylene dyes bearing either anhydrides or carboxy-substituted imides anchor groups were readily attached to inorganic semiconductors such as TiO_2 or ZnO. With these anchoring groups, perylene dyes were utilized as sensitizers in DSSCs.[89] By varying the *bay*- and *peri*- groups, a series of perylene monoimides dyes with tunable colors were achieved. Their absorption overlaps the whole visible region up to the infrared light at 1100 nm.[40] With two additional thiophenyl groups in the bay, the DSSCs of **72** show 87% incident monochromatic photon-to-current conversion efficiency (IPCE) and 6.8% power conversion efficiency under the standard AM 1.5 solar conditions. Up to now, these perylene imides photovoltaic devices showed one of the best efficiencies among perylene-sensitized solar cells.[90] The concept of covalent coupling of perylene imide derivatives to polymers has also been successfully applied in organic LEDs.[91] The emission color of fluorene-based polymers was easily tuned across the whole visible spectrum by copolymerization of perylene dyes. Energy transfer caused the emission stems solely from the dye units which resulted in efficient LEDs. These fluorene-based polymers are suitable of acting as efficient blue, green, or red emitters in full color displays. They might also be blended to produce other emission colors including pure white light.

4.2 Single molecule spectroscopy (SMS)

In contrast to ensemble measurements which yield information on average properties, looking at single molecules provides information on individual molecules such as distributions and time trajectories of properties which can't be obtained by other conventional experiments. In this way, static disorder or dynamic disorder of individual molecules can be detected, which is not possible by averaging the observable of a bulk system. A good fluorophore for such experiments requires a high extinction coefficient, a high fluorescence quantum yield and good chemical and photochemical stability. Photobleaching severely limits observation time and therefore the amount of information obtained from the experiment. Since most PDI and TDI chromophores excellently fulfill all these requirements, they have been adopted as key chromophores for SMS. For tetraphenoxy-substituted PDI, SMS shows conformational changes of the bay substituents resulting from twisting of the single molecule around the central PDI long axis.[39] Besides detection of intrinsic changes within the perylene chromophores, these dyes can also be used to investigate their polymeric environment, e.g. in measuring the free volume of polymers.[92] In dendrimers with multiple identical chromophores, energy hopping and transfer to the chromophore with the energetically lowest singlet state was observed.[56, 93] Either singlet–triplet[56, 94] or singlet–singlet annihilation[95] can occur by excitation of more than one chromophore in one multichoromophores molecule. These annihilation processes are also observed in PDI dimers and are not limited to dendritic systems.[96] The investigation of singlet–singlet and singlet–triplet annihilation is of great importance for constructing single photon sources from organic molecules since their performance strongly relies on these parameters.[97] In addition to the study of photophysical processes in multichromophoric systems with identical chromophores, energy transfer on the single molecule level in donor–acceptor systems consisting of various rylene dyes like the chromophoric triade **96** was also investigated.[98] When the polyphenylene dendrimers at the periphery were functionalized with electron donors instead of energy-donating moieties, reversible electron transfer was observed in single dendritic molecules.[99] Furthermore, by using a delicately designed fluorophore: dinaphtoquaterrylenebis-(dicarboximide) (DNQDI, Figure 9a), not only fluorescence detection for visualization of individual molecules are feasible but experiments on a single molecular level as well. van Hulst and ourselves reported the observation of vibrational wave packets in individual molecules at ambient temperatures by means of the phase-locked spontaneous light emission technique.[100]

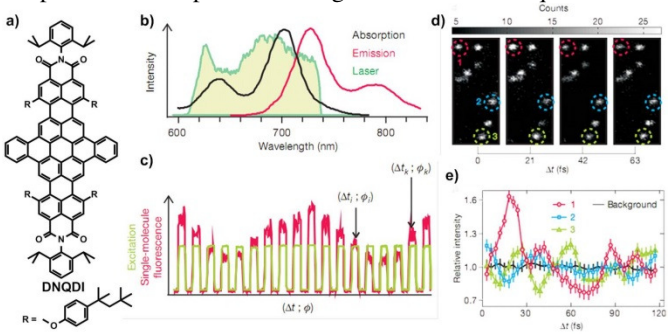

Figure 9. a) Molecualr structure of DNQDI; b) Spectra of DNQDI and broad-band excitation laser used; c) The fluorescence intensity of the single molecules was recorded for different combinations of inter-pulse time delay Δt and phase shift ϕ which were applied sequentially, separated by periods of no illumination and repeated until the molecule photobleached; d) Fluorescence images of single molecules excited with two mutually delayed (Δt), phase-locked laser pulses; **e**) Integrated intensity as a function of Δt for the fluorescence emission of the three molecules marked in d. Adapted with permission from Ref. [100], Copyright 2010, Nature publishing group.

Plotting the integrated fluorescence emission of each molecule (Figure 9c) versus inter-pulse time delay (Δt) reveals an oscillatory behavior of the excitation probability of photoexcitation of the single molecules, which depends on the femtosecond temporal distribution of the photons available for absorption varying from molecule to molecule (Figure 9d, 9e). Such interdependence of the optical and wave-packet phases is the basis for the coherent control of molecular states. Applications of this technique for detecting electronic quantum

coherence or electronic wave packet interferometry in individual pigment-protein complexes will provide further insights into photosynthetic excitation energy transfer.

4.3 Bio-labeling

Single molecule spectroscopy is also a powerful tool for studying biomolecules in aqueous environment.[101] The use of common commercial dyes for this purpose is often limited by their fast photobleaching. Since perylene and terrylene imides possess extraordinary photostability,[1a] they are gaining increasing attention for SMS study in biological systems. For application of higher RDIs in bio-labelling at least two challenges must be faced: as a consequence of their extended aromatic scaffolds, rylene diimides are not soluble in water and relevant buffers. Thus, the introduction of suitable water-solubilizing groups is necessary. Furthermore, after functionalization with hydrophilic substituents, such as sulfonic acid moieties, quaternized amine groups, crown ethers, polyethyleneoxide or peptide chains, the fluorescence of rylene imides usually dramatically decreases or even becomes nonemissive. Thus, making rylene diimides water-soluble and preserving a high fluorescence quantum yield remains a challenging goal for their applications in bio-labeling. Monofunctional rylene dyes were used for non-selective labeling of amino groups in proteins using isothiocyanate or *N*-hydroxysuccinimide esters.[5a] Any free amine in the protein chain can be labeled in this way. For instance, a maleimide

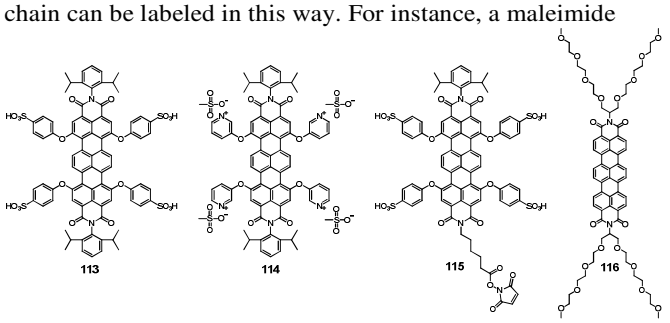

Figure 10. Representative TDI bio-lables **113**-**116**.

group was used for site-specific labeling of enzyme like phospholipase.[5b, 92] It readily reacted with any thiol unit of cystein, either terminal or internal. In contrast, native chemical ligation only bind to terminal cystein groups.[39] As another example, water-soluble rylene imide dyes functionalized with nitrilotriacetic acid moiety do bind to an HIS-tagged protein.[102] Importantly, labelling didn't change the emission of the dye upon complexation with nickel ions. To bridge the gap outside the region of autofluorescence of living cells (> 600 nm), water-soluble TDI derivative **113** carrying sulfonated phenoxy groups were utilized for labeling of single proteins (Figure 10).[5a] The TDI–protein conjugates have been characterized by fluorescence correlation spectroscopy (FCS) and photostability measurements. The uptake of the TDIs in liposomes and in living HeLa cells demonstrated the outstanding capability to label artificial and natural lipid membrane containing compartments. The most striking result in this context is that cellular trafficking of membrane containing compartments, e.g. endosomes in living cells can be observed over very long periods of time (more than 30 min). Control experiments with known dyes acting as fluid phase markers were completely photobleached within 10 s underlining the outstanding properties and future potential of water soluble TDIs for biological applications. Pyridyl substituted TDI **114** was the first reported analogue that didn't form aggregates and thus fluoresced in water, while its photophysical properties were preserved. This strategy of introducing charged substituents into the bay region of rylene imides provided the basis for the application of higher RDIs dyes as bio-labels. The asymmetric functionalization of rylene diimides at the imides structure allowed the introduction of two different kinds of substituents. Therefore a single reactive group for bio-labeling could be attached to this imide position. In this manner, water-soluble TDI dyes with four sulfonic acid groups as well as a single anchoring group allowing bioconjugation with lysine, glutamic acid, or aspartic acid groups was obtained. For example, TDI **115** with maleimide group represents an attractive fluorescent probe for targeting accessible thiol groups in proteins. Another method to avoid aggregation induced fluorescence quenching of rylene imides dyes in water is the formation of micelles promoted by addition of surfactant. For example, our group recently reported a four polyethylene glycol (PEG) chains-modified TDI **116**,[99] which formed soluble non-fluorescing aggregates in water. When incorporated into micelles consisting of 20wt% of block copolymer surfactant (poly(ethylene oxide)-poly-(propylene oxide)-poly-(ethylene oxide) (P123)), most of the TDI **116** molecules were present in monomeric form. Thus, a strong increase in fluorescence was observed. Furthermore, a single-molecule study of TDI **116** in polymeric films of PMMA showed excellent photostability over other commercial water-soluble dyes, such as Rhodamin6G.

5. Conclusion and outlook

Rylene imides dyes are one of the key chromophore systems for various applications. Two of the most investigated representatives are naphthalene imides and perylene imides, owing to their facile synthesis and their extraordinary properties. Higher rylene imide dyes are still in their infancy and have been ignored for quite a long time since their first synthesis. Thus, we summarized the recent development on this specific area and are trying to initiate more research interest and attention to further explore such intriguing dye family.

In this feature article, we have surveyed the recent advances in synthesis of higher rylene imide based materials with an attempt to unveil the underlying design strategies and potential applications. Despite more and more encouraging achievements on development of new synthetic methodologies made by dye chemists, the synthesis of stable NIR absorbed dyes are still not attainable yet. Thus, there is an urgent need in the future to create novel NIR dyes by rational synthetic design and chemical modifications. Furthermore, the synthesis of larger RDIs is restricted due to multi-step synthesis and overall low yields, which prevent larger scale applications. Thus, the main future focus for the synthesis will be on the pursuit of a highly efficient synthetic design method and stabilization strategy based on the fast development of modern synthetic chemistry. Although rylene imides have proven to have enormous potential applications in various fields like OPVs, OFETs, biological labeling, SMS studies etc., a lot of improvements still need to be made. For example, the performance of using rylene diimides as acceptor materials in OPV devices is yet far below the industrial demand. One reasonable direction towards high performance rylene diimides based acceptors is to increase its dimensionality, not only in the π-conjugated molecular structure but also in the direction of intermolecular close-contacts between molecules in the bulk.[103a] A 3D molecular structure together with a network of intermolecular short contacts in three dimensions would make rylene diimides

competitive to fullerenes as acceptor materials in OPVs.[103b] Thus, tremendous efforts from device physicists and material scientists should be efficiently merged to advance in this specific research field.

Acknowledgements

Financial support of this work by BASF AG and VW foundation (AZ.85101-85103), SENSOR are gratefully acknowledged. We also thank Dr. Martin Baumgarten for his help in preparing this manuscript.

Notes and references

[a] Max Planck Institute for Polymer Research, Ackermannweg 10, 55128 Mainz, Germany. E-mail: chen@mpip-mainz.mpg.de; muellen@mpip-mainz.mpg.de; Fax: (+49) 6131-379-350

1. (a) F. Würthner, *Chem. Commun.,* **2004**, 1564-1579; (b) M. R. Wasielewski, *J. Org. Chem.,* **2006**, *71*, 5051-5066; (c) T. Weil, T. Vosch, J. Hofkens, K. Peneva and K. Müllen, *Angew. Chem. Int. Ed*., **2010**, *49*, 9068-9093.
2. A. Herrmann, and Küllen, *Chem. Lett*., **2006**, *35*, 978-985.
3. C. Li and H. Wonneberger, *Adv. Mater*., **2012**, *24*, 613-636.
4. X. Zhan, A. Facchetti, S. Barlow, T. J. Marks, M. A. Ratner, M. R. Wasielewski and S. R. Marder, *Adv. Mater*., **2011**, *23*, 268-284.
5. (a) C. Jung, N. Ruthardt, R. Lewis, J. Michaelis, B. Sodeik, F. Nolde, K. Peneva, K. Müllen and C. Bräuchle, *ChemPhysChem*, **2009**, *10*, 180-190; (b) K. Peneva, G. Mihov, F. Nolde, S. Rocha, J.-i. Hotta, K. Braeckmans, J. Hofkens, H. Uji-i, A. Herrmann and K. Müllen, *Angew. Chem. Int. Ed*., **2008**, *47*, 3372-3375.
6. L. Zang, Y. Che and J. S. Moore, *Acc. Chem. Res*., **2008**, *41*, 1596-1608.
7. P. Dedecker, B. Muls, A. Deres, H. Uji-i, J.-i. Hotta, M. Sliwa, J.-P. Soumillion, K. Müllen, J. Enderlein and J. Hofkens, *Adv. Mater.*, **2009**, *21*, 1079-1090.
8. Z. Chen, A. Lohr, C. R. Saha-Moller and F. Würthner, *Chem. Soc. Rev.,* **2009**, *38*, 564-584.
9. (a) S. V. Bhosale, C. H. Jani and S. J. Langford, *Chem. Soc. Rev*., **2008**, *37*, 331-342; (b) N. Sakai, J. Mareda, E. Vauthey and S. Matile, *Chem. Commun*., **2010**, *46*, 4225-4237; (c) M. R. Wasielewski, *Acc. Chem. Res*., **2009**, *42*, 1910-1921.
10. (a) Y. Avlasevich, C. Li and K. Müllen, *J. Mater. Chem*., **2010**, *20*, 3814-3826; (b) A. C. Grimsdale, K. Müllen, *Angew. Chem. Int. Ed*., **2005**, *44*, 5592-5629; (c) J. Qu, PhD Thesis, Johannes-Gutenberg-University, Mainz, 2004.
11. (a) C. R. Newman, C. D. Frisbie, D. A. da Silva Filho, J.-L. Brédas, P. C. Ewbank and K. R. Mann, *Chem. Mater*., **2004**, *16*, 4436-4451; (b) F. Nolde, W. Pisula, S. Müller, C. Kohl and K. Müllen, *Chem. Mater*., **2006**, *18*, 3715-3725.
12. (a) S. Müller and K. Müllen, *Chem. Commun*., **2005**, 4045-4046; (b) Y. Avlasevich and K. Müllen, *Chem. Commun.*, **2006**, 4440-4442.
13. (a) F. O. Holtrup, G. R. J. Müller, H. Quante, S. De Feyter, F. C. De Schryver and K. Müllen, *Chem. Eur. J*., **1997**, *3*, 219-225; (b) F. Nolde, J. Qu, C. Kohl, N. G. Pschirer, E. Reuther and K. Müllen, *Chem. Eur. J.,* **2005**, *11*, 3959-3967.
14. (a) H. Quante and K. Müllen, *Angew. Chem. Int. Ed*., **1995**, *34*, 1323-1325; (b) Y. Geerts, H. Quante, H. Platz, R. Mahrt, M. Hopmeier, A. Bohm and K. Müllen, *J. Mater. Chem.*, **1998**, *8*, 2357-2369; (c) H. Langhals, G. Schönmann and L. Feiler, *Tetrahedron Lett*., **1995**, *36*, 6423-6424.
15. N. G. Pschirer, C. Kohl, F. Nolde, J. Qu and K. Müllen, *Angew. Chem. Int. Ed*., **2006**, *45*, 1401-1404.
16. K. Tomizaki, P. Thamyongkit, R. S. Loewe and J. S. Lindsey, *Tetrahedron*, **2003**, *59*, 1191-1207.
17. Z. Yuan, S.-L. Lee, L. Chen, C. Li, K. S. Mali, S. De Feyter and K. Müllen, *Chem. Eur. J*., **2013**, *19*, 11842-11846.
18. C. Kohl, S. Becker and K. Müllen, *Chem. Commun*., **2002**, 2778-2779.
19. (a) U. Rohr, P. Schlichting, A. Böhm, M. Gross, K. Meerholz, C. Bräuchle and K. Müllen, *Angew. Chem. Int. Ed.*, **1998**, *37*, 1434-1437; (b) U. Rohr, C. Kohl, K. Müllen, A. van de Craats and J. Warman, *J. Mater. Chem*., **2001**, *11*, 1789-1799; (c) C. Lütke Eversloh, C. Li and K. Müllen, *Org. Lett.,* **2011**, *13*, 4148-4150; (d) W. Jiang, Y. Li, W. Yue, Y. Zhen, J. Qu and Z. Wang, *Org. Lett*., **2009**, *12*, 228-231; (e) H. Usta, C. Newman, Z. Chen and A. Facchetti, *Adv. Mater*., **2012**, *24*, 3678-3684; (f) W. Zhou, F. Jin, X. Huang, X-M. Duan and X. Zhan, *Macromolecules*, **2012**, *45*, 7823-7828; (g) W. Zhou, Z-G. Zhang, L. Ma, Y. Li and X. Zhan, *Sol Energ Mat Sol C*, **2013**, *112*, 13-19.
20. Y. Avlasevich, S. Müller, P. Erk and K. Müllen, *Chem. Eur. J*., **2007**, *13*, 6555-6561.
21. X. Zhang, X. Jiang, K. Zhang, L. Mao, J. Luo, C. Chi, H. S. O. Chan and J. Wu, *J. Org. Chem*., **2010**, *75*, 8069-8077.
22. X. H. Cheng, S. Höger and D. Fenske, *Org. Lett*., **2003**, *5*, 2587-2589.
23. T. Yang, J. Pu, J. Zhang and W. Wang, *J. Org. Chem*., **2013**, *78*, 4857-4866.
24. Z. Zhao, Y. Zhang and Y. Xiao, *J. Org. Chem*., **2013**, *78*, 5544-5549.
25. (a) H. Qian, Z. Wang, W. Yue and D. Zhu, *J. Am. Chem. Soc.*, **2007**, *129*, 10664-10665; (b) Y. Shi, H. Qian, Y. Li, W. Yue and Z. Wang, *Org. Lett*., **2008**, *10*, 2337-2340; (c) H. Qian, F. Negri, C. Wang and Z. Wang, *J. Am. Chem. Soc.*, **2008**, *130*, 17970-17976; (d) Y. Zhen, C. Wang and Z. Wang, *Chem. Commun*., **2010**, *46*, 1926-1928.
26. Y. Zhen, W. Yue, Y. Li, W. Jiang, S. Di Motta, E. Di Donato, F. Negri, S. Ye and Z. Wang, *Chem. Commun*., **2010**, *46*, 6078-6080.
27. W. Yue, A. Lv, J. Gao, W. Jiang, L. Hao, C. Li, Y. Li, L. E. Polander, S. Barlow, W. Hu, S. Di Motta, F. Negri, S. R. Marder and Z. Wang, *J. Am. Chem. Soc*., **2012**, *134*, 5770-5773.
28. L. E. Polander, A. S. Romanov, S. Barlow, D. K. Hwang, B. Kippelen, T. V. Timofeeva and S. R. Marder, *Org. Lett*., **2012**, *14*, 918-921.
29. J. H. Yao, C. Chi, J. Wu and K.-P. Loh, *Chem. Eur. J*., **2009**, *15*, 9299-9302.
30. Q. Bai, B. Gao, Q. Ai, Y. Wu and X. Ba, *Org. Lett*., **2011**, *13*, 6484-6487.
31. Y. Li, W. Xu, S. D. Motta, F. Negri, D. Zhu and Z. Wang, *Chem. Commun*., **2012,** *48*, 8204-8206.
32. C. Lütke Eversloh, Z. Liu, B. Müller, M. Stangl, C. Li and K. Müllen, *Org. Lett*., **2011**, *13*, 5528-5531.
33. C. Huang, S. Barlow and S. R. Marder, *J. Org. Chem*., **2011**, *76*, 2386-2407.
34. H. Qian, C. Liu, Z. Wang and D. Zhu, *Chem. Commun*., **2006**, 4587-4589.

35. H. Qian, W. Yue, Y. Zhen, S. Di Motta, E. Di Donato, F. Negri, J. Qu, W. Xu, D. Zhu and Z. Wang, *J. Org. Chem.*, **2009**, *74*, 6275-6282.
36. C. Jiao, K.-W. Huang, J. Luo, K. Zhang, C. Chi and J. Wu, *Org. Lett.*, **2009**, *11*, 4508-4511.
37. C. Kohl, T. Weil, J. Qu and K. Müllen, *Chem. Eur. J.*, **2004**, *10*, 5297-5310.
38. A. Herrmann, T. Weil, V. Sinigersky, U.-M. Wiesler, T. Vosch, J. Hofkens, F. C. De Schryver and K. Müllen, *Chem. Eur. J.*, **2001**, *7*, 4844-4853.
39. J. Hofkens, T. Vosch, M. Maus, F. Köhn, M. Cotlet, T. Weil, A. Herrmann, K. Müllen and F. C. De Schryver, *Chem. Phys. Lett.*, **2001**, *333*, 255-263.
40. C. Li, J. Schöneboom, Z. Liu, N. G. Pschirer, P. Erk, A. Herrmann and K. Müllen, *Chem. Eur. J.*, **2009**, *15*, 878-884.
41. A. Keerthi, Y. Liu, Q. Wang and S. Valiyaveettil, *Chem. Eur. J.*, **2012**, *18*, 11669-11676.
42. Y. Zagranyarski, L. Chen, Y. Zhao, H. Wonneberger, C. Li and K. Müllen, *Org. Lett*, **2012**, *14*, 5444-5447.
43. Z. Liu, C. Li, M. Wagner, Y. Avlasevich, A. Herrmann and K. Müllen, *Chem. Commun.*, **2008**, 5028-5030.
44. (a) C. G. Hubner, V. Ksenofontov, F. Nolde, K. Müllen and T. Basche, *J. Chem. Phys.*, **2004**, *120*, 10867-10870; (b) B. Fuckel, G. Hinze, G. Diezemann, F. Nolde, K. Müllen, J. Gauss and T. Basche, *J. Chem. Phys.*, **2006**, *125*, 144903-144907.
45. G. Schweitzer, R. Gronheid, S. Jordens, M. Lor, G. De Belder, T. Weil, E. Reuther, K. Müllen and F. C. De Schryver, *J. Phys. Chem. A*, **2002**, *107*, 3199-3207.
46. T. Weil, E. Reuther, C. Beer and K. Müllen, *Chem. Eur. J.*, **2004**, *10*, 1398-1414.
47. C. G. Hubner, V. Ksenofontov, F. Nolde, K. Mullen and T. Basche, *J. Chem. Phys.*, **2004**, *120*, 10867-10870.
48. R. Metivier, F. Nolde, K. Müllen and T. Basche, *Phys. Rev. Lett.*, 2007, 98.
49. H. N. Kim, L. Puhl, F. Nolde, C. Li, L. Chen, T. Basché and K. Müllen, *Chem. Eur. J.*, **2013**, *19*, 9160-9166.
50. C. Curutchet, F. A. Feist, B. Van Averbeke, B. Mennucci, J. Jacob, K. Müllen, T. Basche and D. Beljonne, Phys. *Chem. Chem. Phys.*, **2010**, *12*, 7378-7385.
51. G. Zhou, M. Baumgarten and K. Müllen, *J. Am. Chem. Soc.*, **2007**, *129*, 12211-12221.
52. B. Fuckel, G. Hinze, F. Nolde, K. Müllen and T. Basche, *J. Phys. Chem. A*, **2010**, *114*, 7671-7676.
53. M. Fischer and F. Vögtle, *Angew. Chem. Int. Ed.*, **1999**, *38*, 884-905.
54. K. Inoue, *Prog. Poly. Sci.*, **2000**, *25*, 453-571.
55. (a) K. W. Pollak, J. W. Leon, J. M. J. Fréchet, M. Maskus and H. D. Abruña, *Chem. Mater.*, **1998**, *10*, 30-38; (b) M. S. Matos, J. Hofkens, W. Verheijen, F. C. De Schryver, S. Hecht, K. W. Pollak, J. M. J. Fréchet, B. Forier and W. Dehaen, *Macromolecules*, **2000**, *33*, 2967-2973.
56. J. Hofkens, M. Maus, T. Gensch, T. Vosch, M. Cotlet, F. Köhn, A. Herrmann, K. Müllen and F. De Schryver, *J. Am. Chem. Soc.*, **2000**, *122*, 9278-9288.
57. R. Gronheid, J. Hofkens, F. Köhn, T. Weil, E. Reuther, K. Müllen and F. C. De Schryver, *J. Am. Chem. Soc.*, **2002**, *124*, 2418-2419.
58. T. Christ, F. Kulzer, T. Weil, K. Müllen and T. Basche, *Chem. Phys. Lett.*, **2003**, *372*, 878-885.
59. T. Weil, U. M. Wiesler, A. Herrmann, R. Bauer, J. Hofkens, F. C. De Schryver and K. Müllen, *J. Am. Chem. Soc.*, **2001**, *123*, 8101-8108.
60. T. Vosch, J. Hofkens, M. Cotlet, F. Köhn, H. Fujiwara, R. Gronheid, K. Van Der Biest, T. Weil, A. Herrmann, K. Müllen, S. Mukamel, M. Van der Auweraer and F. C. De Schryver, *Angew. Chem. Int. Ed.*, **2001**, *40*, 4643-4648.
61. J. Wu, W. Pisula and K. Müllen, *Chem. Rev.*, **2007**, *107*, 718-747.
62. J. Wu, J. Qu, N. Tchebotareva and K. Müllen, *Tetrahedron Lett.*, **2005**, *46*, 1565-1568.
63. B. Fückel, G. Hinze, J. Wu, K. Müllen and T. Basché, *ChemPhysChem*, **2012**, *13*, 938-945.
64. (a) N. K. S. Davis, M. Pawlicki and H. L. Anderson, *Org. Lett.*, **2008**, *10*, 3945-3947; (b) N. K. S. Davis, A. L. Thompson and H. L. Anderson, *Org. Lett.*, **2010**, *12*, 2124-2127; (c) N. K. S. Davis, A. L. Thompson and H. L. Anderson, *J. Am. Chem. Soc.*, **2010**, *133*, 30-31.
65. L. Zeng, C. Jiao, X. Huang, K.-W. Huang, W.-S. Chin and J. Wu, *Org. Lett.*, **2011**, *13*, 6026-6029.
66. C. Jiao, L. Zhu and J. Wu, *Chem. Eur. J.*, **2011**, *17*, 6610-6614.
67. S. Shimizu, T. Iino, Y. Araki and N. Kobayashi, *Chem. Commun.*, **2013**, *49*, 1621-1623.
68. C. Jiao, K.-W. Huang, Z. Guan, Q.-H. Xu and J. Wu, *Org. Lett.*, **2010**, *12*, 4046-4049.
69. C. Jiao, N. Zu, K.-W. Huang, P. Wang and J. Wu, *Org. Lett.*, **2011**, *13*, 3652-3655.
70. D. Désilets, P. M. Kazmaier and R. A. Burt, *Can. J. Chem.*, **1995**, *73*, 319-324.
71. Y. Ruiz-Morales, *J. Phys. Chem. A*, **2002**, *106*, 11283-11308.
72. (a) Z. Sun, K.-W. Huang and J. Wu, *Org. Lett.*, **2010**, *12*, 4690-4693; (b) Z. Sun, K.-W. Huang and J. Wu, *J. Am. Chem. Soc.*, **2011**, *133*, 11896-11899.
73. M. R. Hansen, T. Schnitzler, W. Pisula, R. Graf, K. Müllen and H. W. Spiess, *Angew. Chem. Int. Ed.*, **2009**, *48*, 4621-4624.
74. H. N. Tsao, W. Pisula, Z. Liu, W. Osikowicz, W. R. Salaneck and K. Müllen, *Adv. Mater.*, **2008**, *20*, 2715-2719.
75. (a) L. Schmidt-Mende, A. Fechtenkötter, K. Müllen, E. Moons, R. H. Friend and J. D. MacKenzie, *Science*, **2001**, *293*, 1119-1122; (b) J. L. Li, M. Kastler, W. Pisula, J. W. F. Robertson, D. Wasserfallen, A. C. Grimsdale, J. S. Wu and K. Müllen, *Adv. Funct. Mater*, **2007**, *17*, 2528-2533.
76. L. F. Dössel, V. Kamm, I. A. Howard, F. Laquai, W. Pisula, X. Feng, C. Li, M. Takase, T. Kudernac, S. De Feyter and K. Müllen, *J. Am. Chem. Soc.*, **2012**, *134*, 5876-5886.
77. K. S. Mali, J. Adisoejoso, E. Ghijsens, I. De Cat and S. De Feyter, *Acc. Chem. Res.*, **2012**, *45*, 1309-1320.
78. (a) Q. H. Wang and M. C. Hersam, Nat Chem, 2009, 1, 206-211; (b) H. Huang, S. Chen, X. Gao, W. Chen and A. T. S. Wee, *ACS Nano*, **2009**, *3*, 3431-3436.
79. (a) B. Yoo, T. Jung, D. Basu, A. Dodabalapur, B. A. Jones, A. Facchetti, M. R. Wasielewski and T. J. Marks, *App. Phys. Lett.*, **2006**, *88*, 082104-082103; (b) J. E. Anthony, A. Facchetti, M. Heeney, S. R. Marder and X. Zhan, *Adv. Mater.*, **2010**, *22*, 3876-3892; (c) X. Zhao and X. Zhan, *Chem. Soc. Rev.*, **2011**, *40*, 3728-3743.
80. (a) M. A. Angadi, D. Gosztola and M. R. Wasielewski, *J. Appl. Phys.*, **1998**, *83*, 6187-6189; (b) X. Zhan, Z. Tan, B. Domercq, Z. An, X.

Zhang, S. Barlow, Y. Li, D. Zhu, B. Kippelen and S. R. Marder, *J. Am. Chem. Soc.*, **2007**, *129*, 7246-7247; (c) Y. Lin, Y. Li and X. Zhan, *Chem. Soc. Rev.*, **2012**, *41*, 4245-4272; (d) P. Cheng, L. Ye, X. Zhao, J. Hou, Y. Li and X. Zhan, *Energy Environ. Sci*. **2014**, DOI:10.1039/C3EE43041C.

81. Z. Chen, M. G. Debije, T. Debaerdemaeker, P. Osswald and F. Würthner, *ChemPhysChem*, **2004**, *5*, 137-140.
82. S. Tatemichi, M. Ichikawa, T. Koyama and Y. Taniguchi, *App. Phys. Lett*., **2006**, *89*, 112108-112103.
83. A. S. Molinari, H. Alves, Z. Chen, A. Facchetti and A. F. Morpurgo, *J. Am. Chem. Soc*., **2009**, *131*, 2462-2463.
84. C. W. Tang, *App. Phys. Lett*., 1986, 48, 183-185.
85. A. Sharenko, C. M. Proctor, T. S. van der Poll, Z. B. Henson, T.-Q. Nguyen and G. C. Bazan, *Adv. Mater*., **2013**, *25*, 4403-4406.
86. W. Pisula, M. Kastler, D. Wasserfallen, J. W. F. Robertson, F. Nolde, C. Kohl and K. Müllen, *Angew. Chem. Int. Ed*., **2006**, *45*, 819-823.
87. J. Li, F. Dierschke, J. Wu, A. C. Grimsdale and K. Müllen, *J. Mater. Chem.,* **2006**, *16*, 96-100.
88. A. Mishra, C.-Q. Ma and P. Bäuerle, *Chem. Rev*., **2009**, *109*, 1141-1276.
89. H. Tian, P.-H. Liu, F.-S. Meng, E. Gao and S. Cai, *Syn. Metal*., **2001**, *121*, 1557-1558.
90. (a) T. Edvinsson, C. Li, N. Pschirer, J. Schöneboom, F. Eickemeyer, R. Sens, G. Boschloo, A. Herrmann, K. Müllen and A. Hagfeldt, J. *Phys. Chem. C*, **2007**, *111*, 15137-15140; (b) C. Li, J.-H. Yum, S.-J. Moon, A. Herrmann, F. Eickemeyer, N. G. Pschirer, P. Erk, J. Schöneboom, K. Müllen, M. Grätzel and M. K. Nazeeruddin, *ChemSusChem*, **2008**, *1*, 615-618.
91. C. Ego, D. Marsitzky, S. Becker, J. Zhang, A. C. Grimsdale, K. Müllen, J. D. MacKenzie, C. Silva and R. H. Friend, *J. Am. Chem. Soc*., **2002**, *125*, 437-443.
92. R. A. L. Vallée, M. Cotlet, M. Van Der Auweraer, J. Hofkens, K. Müllen and F. C. De Schryver, *J. Am. Chem. Soc.*, **2004**, *126*, 2296-2297.
93. W. Schroeyers, R. Vallée, D. Patra, J. Hofkens, S. Habuchi, T. Vosch, M. Cotlet, K. Müllen, J. Enderlein and F. C. De Schryver, *J. Am. Chem. Soc*., **2004**, *126*, 14310-14311.
94. T. Vosch, M. Cotlet, J. Hofkens, K. Van Der Biest, M. Lor, K. Weston, P. Tinnefeld, M. Sauer, L. Latterini, K. Müllen and F. C. De Schryver, *J. Phys. Chem. A*, **2003**, *107*, 6920-6931.
95. P. Tinnefeld, K. D. Weston, T. Vosch, M. Cotlet, T. Weil, J. Hofkens, K. Müllen, F. C. De Schryver and M. Sauer, *J. Am. Chem. Soc*., **2002**, *124*, 14310-14311.
96. C. G. Hübner, G. Zumofen, A. Renn, A. Herrmann, K. Müllen and T. Basché, *Phys. Rev. Lett*., **2003**, *91*, 093903.
97. T. D. M. Bell, J. Jacob, M. Angeles-Izquierdo, E. Fron, F. Nolde, J. Hofkens, K. Mullen and F. C. D. Schryver, *Chem. Commun*., **2005**, 4973-4975.
98. (a) M. Cotlet, R. Gronheid, S. Habuchi, A. Stefan, A. Barbafina, K. Müllen, J. Hofkens and F. C. De Schryver, *J. Am. Chem. Soc*., **2003**, *125*, 13609-13617; (b) R. Métivier, F. Kulzer, T. Weil, K. Müllen and T. Basché, *J. Am. Chem. Soc.*, **2004**, *126*, 14364-14365; (c) M. Cotlet, T. Vosch, S. Habuchi, T. Weil, K. Müllen, J. Hofkens and F. De Schryver, *J. Am. Chem. Soc*., **2005**, *127*, 9760-9768.
99. M. Cotlet, S. Masuo, G. Luo, J. Hofkens, M. Van der Auweraer, J. Verhoeven, K. Müllen, X. S. Xie and F. De Schryver, *Prof. Natl. Acad. Sci. USA*, **2004**, *101*, 14343-14348.
100. D. Brinks, F. D. Stefani, F. Kulzer, R. Hildner, T. H. Taminiau, Y. Avlasevich, K. Müllen and N. F. van Hulst, *Nature*, **2010**, 465, 905-908.
101. E. J. G. Peterman, H. Sosa and W. E. Moerner, *Annu. Rev. Phys. Chem.*, **2004**, *55*, 79-96.
102. K. Peneva, G. Mihov, A. Herrmann, N. Zarrabi, M. Börsch, T. M. Duncan and K. Müllen, *J. Am. Chem. Soc*., **2008**, *130*, 5398-5399.
103. a) P. J. Skabara, J-B. Arlin, and Y. H. Geerts, *Adv. Mater*., **2013**, *25*, 1948-1954; b) W. Jiang, L. Ye, X. Li, C. Xiao, F. Tan, W. Zhao, J. Hou, and Z. Wang, *Chem. Commun*., **2014**, *50*, 1024-1026.